NUCLEAR MATTER WITH COUPLED CLUSTER THEORY

by

JOHANNES A. REKKEDAL

THESIS

for the degree of

MASTER OF SCIENCE

(Master in Computational physics)

Faculty of Mathematics and Natural Sciences
Department of Physics
University of Oslo

Det matematisk- naturvitenskapelige fakultet
Universitetet i Oslo

Acknowledgements

First of all I have to thank my wife Nubia and my family for being so patient with me in this stressful time.

I would like to thank my supervisor Morten Hjorth-Jensen. I am very grateful for all the help and guidance he has given me during my two years as a master student.

I am very grateful for my fellow students. I would like to thank the people sharing the office with me, Rune, Lene, Patrick and Islen. I would especially thank Gustav Jansen for reviewing the chapter on coupled cluster theory and for some interesting discussions at Oak Ridge.

Finally I have to thank Jan Lindroos for reviewing the thesis and for all the interesting discussion we have had about everything regarding physics and mathematics.

Notation

Units

We will in all chapters except the second, regarding quantum mechanics, work with units, where

$$\hbar = c = 1$$

In this system,

$$\text{[length]} = \text{[time]} = \text{[energy]}^{-1} = \text{[mass]}^{-1}.$$

The mass m of a particle is therefore equal to its rest energy (mc^2).

Vectors

Vectors are boldfaced, $\mathbf{v}$ is an ordinary vector in three dimensions. Four vectors are denoted by a Greek letter, A^μ, where $\mu = (0, 1, 2, 3)$

$$A^\mu = \left(A^0, \mathbf{A}\right) \text{ and } A_\mu = (-A^0, \mathbf{A})$$

Summation convention

We use Einstein summation conventions, where equal upper and lower indices are summed over, Greek letters are summed from zero to three,

$$A^\mu B_\mu = \sum_{\mu=0}^{3} A^\mu B_\mu.$$

Spin and isospin

The Pauli spin matrices σ are defined as

$$\sigma^i = \begin{pmatrix} 0 & 1 \\ 1 & 0 \end{pmatrix}, \ \sigma^j = \begin{pmatrix} 0 & -i \\ i & 0 \end{pmatrix} \text{ and } \sigma^k = \begin{pmatrix} 1 & 0 \\ 0 & -1 \end{pmatrix}.$$

The isospin matrices τ are defined as

$$\tau^i = \begin{pmatrix} 0 & 1 \\ 1 & 0 \end{pmatrix}, \ \tau^j = \begin{pmatrix} 0 & -i \\ i & 0 \end{pmatrix} \text{ and } \tau^k = \begin{pmatrix} 1 & 0 \\ 0 & -1 \end{pmatrix}.$$

Commutators

A commutator between two operators A and B is defined as

$$[A, B] = AB - BA.$$

The anticommutator is defined as

$$\{A, B\} = AB + BA.$$

Contents

Chapter 1

Introduction

In 1967 the first pulsar was observed [1], and based on characteristic observational features this object was identified as a neutron star. After direct evidences of the existence of neutron stars, nuclear models have been widely employed in the description of the internal structure of neutron stars. It turned out that the equation of state of nuclear matter is not only a very important ingredient in the study of nuclear properties and heavy ion collisions, but also in studies of neutron stars and supernovae.

Nuclear matter is an idealized system with an infinite amount of nucleons and contains an equal amount of protons and neutrons. Even though it is a theoretical construct it is possible to obtain some "experimental" values regarding nuclear matter, such as the binding energy per nucleon and the saturation density, ρ_0, which is a function of the Fermi momentum k_f. This is obtained by using the semi-empirical mass formula and divide by the nucleon number, A, letting A go to infinity. A main purpose of nuclear matter theories is to derive the binding energy per nucleon by first principles. Following this approach one can determine the nuclear matter density ρ_0 and the incompressibility coefficient K which relates to the equation of state through

$$K = \Big[k^2 \frac{d^2}{dk^2}(\frac{\varepsilon}{\rho})\Big] = 9\Big[\rho^2 \frac{d^2}{d\rho^2}(\frac{\varepsilon}{\rho})\Big],$$

where ε denotes the energy density, ρ is the Baryonic density and k denotes the momenta. The incompressibility coefficient defines the curvature of the equation of state $\varepsilon(\rho)/\rho$ at ρ_0.

There are many theoretical reasons that motivate the use of coupled cluster. The method is fully microscopic. When one expands the cluster operator in coupled cluster theory to all particles in a system, one reproduces the full correlated many-body wavefunction of the system. The coupled cluster method is size consistent, the energy of two noninteracting fragments computed separately is the same as computing

the energy for both systems simultaneously. Furthermore, the coupled cluster method is size extensive, the energy computed scales linearly with the number of particles. A size extensive method is often defined as a method where there are no unlinked diagrams in the energy and amplitude equations. The coupled cluster method is not variational, however the energy tends to behave as a variational quantity in most instances.

The aim of the thesis is to do nuclear matter calculations with the coupled cluster method. We calculate the binding energy for nuclear matter.

This is not the first work on nuclear matter, different many-body methods such as Hartree-Fock calculations and perturbation theory have also been performed on nuclear matter. However a perturbative approach is difficult because of the repulsive core in the nucleon-nucleon interaction. This difficulty has been circumvented by using Brüeckner's method, by defining the so-called Brüeckner G-matrix. Even the coupled cluster method has been used to calculate properties of nuclear matter as done in Ref. [2].

In our calculations the interaction-elements are given in laboratory coordinates and the wavefunction expanded in partial waves.The calculations were done in a plane wave basis in the laboratory system, by using transformation brackets described by Kung in Ref. [3]. When operating in a plane wave basis it is necessary integrate over the momenta. The numerical integration was done by using twelve mesh points, six mesh points for holes and six for particles. As we wanted a more theoretical approach to the problem we chose to use the interactions derived from the chiral symmetries of QCD, N^{3}LO with the scale $\Lambda = 500$ MeV, rather than using the more phenomenological ones. The N^{3}LO potential was further renormalized with a similarity transformation method, resulting in a so-called low-momentum interaction V_{low-k}. We wanted to calculate with at least three cutoffs, $\lambda = 2.1$, $\lambda = 2.2$ fm^{-1} and $\lambda = 2.5$ fm^{-1}.

We managed to calculate energies for the cutoffs at $\lambda = 2.1$ fm^{-1} and $\lambda = 2.2$ fm^{-1}. With the cutoff $\lambda = 2.5$ fm^{-1} we were just able to compute the energy for one k_f value, because of both time limits and convergence problems.

Outline

Large parts of the thesis contain a description of the theoretical prerequisites. The first chapter gives a brief review of quantum mechanics, which is thought to be a

natural theory to include. Instead of giving a mathematical definition of quantum mechanics we preferred to write more about the philosophical interpretations of it, such that not only physicists will enjoy reading it. The following chapter gives a short overview of second quantization which culminates in normal ordering the Hamilton operator, a feature which is crucial in the coupled cluster calculations. Since we are doing a many-body calculation we found it rather important to include a chapter on perturbation theory. Actually, some of the diagrams obtained in the perturbative approach are similar to the ones in the coupled cluster approach. Since we are doing calculations of nuclear matter we felt it impossible not to write about the nuclear force, and we go quickly through chiral perturbation theory since we are using interactions derived from it. Chiral perturbation theory is a rather hard subject and the author admits that he is still not acquainted with it. Of course there is also a chapter only dedicated to the coupled cluster method. We have tried to write most of the derivations, since it is not uncommon to become rather frustrated when writers leave out crucial derivations in their books. We refer to other texts whenever parts of the derivations are left out, especially Ref. [4] for which chapter 7 is based on. The final part concerns the results of the calculations.

Chapter 2

Some historical aspects regarding quantum mechanics

It is not easy to give a short presentation of quantum mechanics, it is a rather huge and strange subject. When speaking about quantum mechanics we should always keep in mind what Feynman said, ”I think it is safe to say that no one understands Quantum Mechanics”. The world quantum mechanics treats, is a small world, the world of very small objects, such as electrons, atoms and nuclei.

The most natural point to start when reviewing quantum mechanics is maybe how it started. It started with light, the feature of light has long been an important part in physics. The explanation of light has long been alternating between the definition of light as a wave picture and a corpuscular picture. Light has interested man in maybe all of time. The Iraqi born scientist Ibn al-Haytham (965-1040), which in the west goes under the name Alhazen, in his Book of optics, treats light as energy particles that travel in straight lines at a high but finite speed [5]. Issac Newton followed the particle interpretation of light, however he understood that he had to associate light with waves in order to explain the diffraction properties of light. Robert Hooke and Christian Huygens believed light to be waves and worked out their own and separate theories of light.

In our everyday life we can see a clear distinction between waves and particles, waves exhibit a phenomena called interference which particles do not. Interference occurs when two waves traveling in the same medium meet. As an example we can look at two sine waves traveling in opposite directions and with the same amplitude. If these two waves meet when both are on their maxima the net result of the waves will be a peak with twice the amplitude of the waves, which is an example of constructive interference. If the waves are completely out of phase when they meet, one of the waves is phasing upwards and the other downwards, the net result will be a zero peak,

this type of interference is called destructive. There will be constructive interference when the displacement of the two waves are in the same direction and destructive when the displacement of the waves are in opposite directions.

There are two experiments which are rather crucial in quantum mechanics, and revolutionized physics. The photoelectric effect, explained by Einstein, for which he got the Nobel prize and the double-slit experiment. In the photoelectric effect light is scattered on metal and collides with the electrons. The collisions can be registered by measuring the current. If light were to be a wave the average energy measured of a single electron should increase with the intensity, the phenomena observed was a surprise. The energy of the ejected electrons did not at all depend on the intensity. It was found that it depends on the frequency of the light waves, and that below a certain frequency there were no ejected electrons. Einstein resolved this paradox by proposing that light consists of individual quanta, which now are called photons. These photons carry energies which come in discrete quanta. The energy can just come in amounts of $\hbar\omega$, where $\hbar$ goes under the name of Planck's constant, and ω is the frequency of the light. By varying the frequency of light it was also discovered that the momentum p is proportional to the wavenumber k and a multiple of planck's constant, $p = \hbar k$. With these expressions of energy and momentum it was deduced from Einstein's famous equation for energy $E = \sqrt{p^2c^2 + m^2c^4}$ that the photon is massless.
The double slit experiment with light shows the opposite behavior. In the double slit experiment light waves are send in a way such that they are incident normally on a screen with two slits S_1 and S_2, which are a distance a apart. If only slit S_1 is open an intensity pattern I_1, is observed. And likewise if only S_2 is open an intensity pattern I_2 is observed. When both of the slits are left open an interference pattern is observed, what is crucial is that the intensity I_{1+2} is not $I_1 + I_2$ which would be the case if light were to be particles.

This seemingly contradictory properties of light was then interpreted as the particle wave duality of light. The Copenhagen interpretation, which states that particles such as photons, but also electrons and other small particles have both wave and particle properties. The particles obey a complementary principle which states that an experiment can show particle like properties and another wave like properties, but none can show them both at the same time. This is the most accepted interpretation of quantum mechanics, however Einstein has always questioned this interpretation and together with Podolsky and Rosen proposed a paradox later called the EPR paradox. We will not go through this paradox, it can be read in any book treating quantum theory. When Aspect did experiments on Bell's inequalities, he showed the consistency of the Copenhagen interpretation. However Afshar claims that he in a recent experiment has showed both particle and wave properties at the same time, Refs. [6, 7].

Now the time has come to say something about the postulates and mathematics of quantum mechanics. The first postulate is that the state of a particle is represented by a vector, or ket $|\Psi(t)\rangle$ in the Hilbert space, $\mathcal{H}$. All properties of the particle are contained in this wave function. Properties of the particles which can be measured, such as position, energy and velocity are in quantum mechanics called observables and are represented by operators. If a particle is in a state $|\Psi\rangle$, the measurement of a variable O, will yield us one of the eigenvalues o. The probability that the eigenvalue o is measured is $|\langle o|\Psi\rangle|^2$. After the measurement, the state of the system changes from the state $|\Psi\rangle$ to the state $|o\rangle$. This effect is called the collapse of the state. Complications caused by the collapse of the wave function arise when measuring different observables. If we measure an observable λ, just after the observable ω is measured we are not generally expected to get an accurate value of λ. When we measure ω the wave function collapses to the eigenfunction corresponding to the eigenvalue we get for its corresponding operator Ω. The condition for getting an accurate value for both of the observables is that theirs corresponding operators commute

$$[\Omega, \Lambda] = \Omega\Lambda - \Lambda\Omega = 0.$$

If two operators do not commute they form a different set of eigenfunctions, and we cannot measure both eigenvalues without an uncertainty. The least uncertainty is the value $[\Omega, \Lambda]$. As an example of two operators that do not commute are the two operators of position and momentum, $[X, P] = i\hbar$.

The last postulate treats the state's evolution with time. All states obey the Schrödinger equation

$$i\hbar\frac{d}{dt}|\Psi(t)\rangle = H|\Psi(t)\rangle, \tag{2.1}$$

where H is the Hamiltonian operator whose eigenvalue denotes the energy of the system. When we are considering a system we use the classical Hamiltonian, but change all the observables to operators. For instance the Hamiltonian describing a classical harmonic oscillator is

$$H = \frac{p^2}{2m} + \frac{1}{2}m\omega^2 x^2,$$

while in quantum mechanics it is on the form

$$H = \frac{P^2}{2m} + \frac{1}{2}m\omega^2 X^2,$$

where P is the momentum operator and X the position operator. When we work in coordinate space the momentum operator becomes a differential operator $P =$

$-i\hbar\nabla$. Since H is an operator it should have an eigenvalue and an eigenstate. This has to be used in order to find the state of a particle. We have to solve the equation

$$H|\Psi(t)\rangle = E|\Psi(t)\rangle,$$

where the energy E is the eigenvalue corresponding to the eigenket $|\Psi(t)\rangle$. It is not always easy to solve the Schrödinger equation since it is a differential equation and when we have to solve a many body problem it may seem impossible.

Chapter 3

Second Quantization

Doing nuclear physics is actually studying many-particle systems. Direct solution of the Schrödinger equation in configuration space is impractical[8] and, even more, it may seem impossible to solve, as mentioned in the last chapter. Such difficulties derives from the terms related to the interparticle potential. However, the second quantization method has turned out to be a helpful and practical tool when treating many-body physics.

In second quantization one define the so-called creation $a^\dagger_\alpha$ and annihilation a_α operators, which create and annihilate a particle, respectively. The subscript α indicates the set of quantum numbers a particle has and it defines what usually is called a single-particle state.

The system studied in this thesis consists of nucleons which belong to the type of particles called fermions. Fermions are particles with half integer spin. In order to obey the Pauli exclusion principle[1], a system consisting of such particles is described by an antisymmetric wave function. On the other hand, the Hamiltonian takes the form

$$H = \sum_{k=1}^{N} t(x_k) + \frac{1}{2} \sum_{k \neq l=1}^{N} v(x_k, x_l), \tag{3.1}$$

where t and v represent the kinetic and potential energy, respectively. x_k denotes the coordinates of particle k.

The factor $1/2$ in the equation above arises from the fact that the potential energy term represents the interaction between every pair of particles, counted once, see for example Ref. [8]. Therefore, we need to include it, in order to not double count.

[1]The Pauli principle states that two identical fermions cannot have the same set of quantum numbers, ie. they cannot be in the same single particle state.

3.1 Creation and annihilation operators

The interpretation of occupation of the antisymmetric many-body fermion states allow us to introduce the two operators $a_\alpha^\dagger$ and a_α, which create and annihilate a particle in the single particle state α, which can be expressed as

$$a_\alpha^\dagger|0\rangle = |\alpha\rangle \text{ and } a_\alpha|\alpha\rangle = |0\rangle \tag{3.2}$$

respectively. The state vector $|0\rangle$ indicates the true vacuum. The algebra of these operators depends on whether the system under consideration is one of bosons or fermions. Bosons obey the commutation relations

$$[a_k, a_{k'}^\dagger] = \delta_{k,k'} \text{ and } [a_k, a_{k'}] = [a_k^\dagger, a_{k'}^\dagger] = 0, \tag{3.3}$$

while for the fermion case yields the following anti-commutation relations

$$\{a_k, a_{k'}^\dagger\} = \delta_{k,k'} \text{ and } \{a_k, a_{k'}\} = \{a_k^\dagger, a_{k'}^\dagger\} = 0, \tag{3.4}$$

where

$$\delta_{k',k} = \begin{cases} 1 & \text{if } k' = k \\ 0 & \text{otherwise.} \end{cases}$$

With the above expressions for the commutators and anti-commutators regarding the creation and annihilation operators the many-body Hamiltonian[2] can be written as

$$H = \sum_{ik} t_{ki} a_k^\dagger a_i + \frac{1}{2} \sum_{ijkl} v_{ijkl} a_i^\dagger a_j^\dagger a_l a_k. \tag{3.5}$$

When the operators in the second quantization are non-relativistic and conserve the particle number, there should be an equal amount of creation and destruction operators in the Hamiltonian. A second quantized many-body operator is written as a sum of one-particle operators, an operator that acts on one particle at a time as in Eq. (3.6)

$$F = \sum_{\alpha,\beta} \langle\alpha|f|\beta\rangle a_\alpha^\dagger a_\beta, \tag{3.6}$$

and as a sum of two-particle operators in the form

$$V = \frac{1}{2} \sum_{\alpha\beta\gamma\delta} \langle\alpha\beta|v|\gamma\delta\rangle a_\alpha^\dagger a_\beta^\dagger a_\delta a_\gamma. \tag{3.7}$$

By using creation and annihilation operators we are able to write down a many-body

[2] Many-body operators are denoted by capital letters in this text.

wave-function (denoted by capital Greek letters) in contrast to single-particle states (denoted by small Greek letters). A wave function consisting of N particles is written as a product of N creation operators,

$$|\Phi\rangle = a_1^\dagger a_2^\dagger a_3^\dagger \cdots a_N^\dagger |0\rangle$$

Here x_i for $i = 1, \ldots, N$ refers to the coordinates of particle number i, the ket vector $|0\rangle$ still indicates the true vacuum and the subscript of the creation operator refers to the single particle state the particle occupies. The problem with this definition of the many-body wave function is that it is not a symmetry eigenstate. By quantum mechanics every particle should be able to occupy every single-particle state, φ_i, with a probability p. Since we now are dealing only with fermions, the total wave-function should be antisymmetric by the interchange of two particles. This requirement is fullfiled by a Slater-determinant, as known in the many body jargon,

$$\frac{1}{\sqrt{N!}} \begin{vmatrix} \varphi_i(x_1) & \varphi_j(x_1) & \varphi_k(x_1) & \varphi_l(x_1) & \cdots & \varphi_N(x_1) \\ \varphi_i(x_2) & \varphi_j(x_2) & \varphi_k(x_2) & \varphi_l(x_2) & \cdots & \varphi_N(x_2) \\ \varphi_i(x_3) & \varphi_j(x_3) & \varphi_k(x_3) & \varphi_l(x_3) & \cdots & \varphi_N(x_3) \\ \varphi_i(x_4) & \varphi_j(x_4) & \varphi_k(x_4) & \varphi_l(x_4) & \cdots & \varphi_N(x_4) \\ \vdots & \vdots & \vdots & \vdots & \vdots & \vdots \\ \varphi_i(x_N) & \varphi_j(x_N) & \varphi_k(x_N) & \varphi_l(x_N) & \cdots & \varphi_N(x_N) \end{vmatrix}. \tag{3.8}$$

A more handy form to write the wave function, is as a permutation of every possible single-particle states φ_i. We rewrite the many-body wave-function as

$$|\Phi\rangle = \prod_{\substack{ij=1, \\ i \neq j}}^{N} P(ij) a_1^\dagger a_2^\dagger a_3^\dagger \cdots a_N^\dagger |0\rangle.$$

The permutation operator $P(ij)$ is defined as when acting on $a_i^\dagger a_j^\dagger$ gives $-a_i^\dagger a_j^\dagger$.

3.2 Wick's Theorem

A normal ordered second quantized operator is defined as an operator whose annihilation operators stands to right of all creation operators. It is in some manner easier to calculate when the annihilation operators are placed to the right. Wick's theorem describes a fast method to put the annihilation operators to the right of the creation operators, by using the anti commutation rules for these operators. Before introducing Wick's theorem we present some definitions like the normal product of operators and contractions of operators.

Given a product of creation and annihilation operators $XYZ\cdots W$, the normal product is defined as

$$N(XYZ\cdots W),$$

where all the destruction operators are moved to the right of the creation operators. As an example let us study the cases

$$N(a_\alpha^\dagger a_\beta) = a_\alpha^\dagger a_\beta \tag{3.9}$$

and

$$N(a_\alpha a_\beta^\dagger) = \pm a_\beta^\dagger a_\alpha, \tag{3.10}$$

where the minus sign applies for fermions only, and the plus sign for bosons.

One of the properties of a normal ordered product of operators is that the vacuum expectation value of the product is zero, the destruction operator annihilates the vacuum state.

A contraction of two operators XY is defined as its expectation value regarding the vacuum, $|0\rangle$,

$$\overbrace{a_\alpha a_\beta^\dagger} = \langle 0|a_\alpha a_\beta^\dagger|0\rangle = \langle 0|\delta_{\alpha\beta} - a_\beta^\dagger a_\alpha|0\rangle = \delta_{\alpha\beta}. \tag{3.11}$$

By having defined the normal product and the contraction in Eq. (3.11) we are now ready to state Wick's theorem which says that a product of randomly oriented creation and annihilation operators can be written as the normal product of these operators plus the normal product of all possible contractions.

$$XYZ\cdots W = N(XYZ\cdots W) + \sum_{\text{contractions}}^{\text{all possible}} N(XYZ\cdots W). \tag{3.12}$$

As a remark, in this theorem only fermions have been considered. The proof of this theorem can be found in almost all books that treat quantum field theory or quantum theory of many-particles, see for example Ref. [9].

3.3 The Particle-Hole Formalism

In a theory of many-particles, it is often more convenient to use another state as reference rather than the vacuum. It should be a stable state. The normal ordering will then be altered from the one given above for the true vacuum state, it is written $|\Phi_0\rangle = a_i^\dagger a_j^\dagger \cdots |0\rangle$. A new definition of the creation and destruction operators is

needed. The operators will now create and annihilate holes and particles. The definition of a hole is a one-particle state that is occupied in the reference state $|\Phi_0\rangle$, while a particle state is a one-particle state that is not occupied in $|\Phi_0\rangle$. This new nomenclature is easily understood when considering that a "hole" is created when an originally occupied state is acted upon by an annihilation operator such as a_i. A "particle" is created when an unoccupied state is acted upon by a creation operator. These operators that destroy and create holes and particles are called quasiparticle operators. A q-annihilation operator annihilates holes and particles, while a q-creation operator creates holes and particles.

A normal ordered product of quasiparticle operators would then be defined as a product where all the quasiparticle destruction operators stand to the right of all the quasiparticle creation operators. This definition of the normal ordered product changes the analysis of Wick's theorem. The only contractions that contribute are the ones where a destruction operator stands to the left of a creation operator, there are two ways this can happen

$$\begin{aligned} \overbrace{a_i^\dagger a_j} &= a_i^\dagger a_j - N(a_i^\dagger a_j) = a_i^\dagger a_j + a_j a_i^\dagger = \delta_{ij} \\ \overbrace{a_i a_j^\dagger} &= a_i a_j^\dagger - N(a_i a_j^\dagger) = a_i a_j^\dagger + a_j^\dagger a_i = \delta_{ij}. \end{aligned} \tag{3.13}$$

That is if i defines a hole state in Eqs. (3.13). As an example, consider normal ordering of a two particle Hamiltonian, as in the following equation

$$\hat{H} = \sum_{pq} \langle p|h|q\rangle a_p^\dagger a_q + \frac{1}{4}\sum_{pqrs}\langle pq|V|rs\rangle a_p^\dagger a_q^\dagger a_s a_r \tag{3.14}$$

The one-particle part is written as

$$\sum_{pq}\langle p|h|q\rangle N(a_p^\dagger a_q) + \sum_{i\in hole}\langle i|h|i\rangle. \tag{3.15}$$

The two-particle part is rewritten as

$$\begin{aligned} &\frac{1}{4}\sum_{pqrs}\langle pq|V|rs\rangle a_p^\dagger a_p^\dagger a_s a_r = \frac{1}{4}\sum_{pqrs}\langle pq|V|rs\rangle N(a_p^\dagger a_q^\dagger a_s a_r) + \\ &\sum_{ipq}\langle pi|V|qi\rangle N(a_p^\dagger a_r) + \frac{1}{2}\sum_{ij}\langle ij|V|ij\rangle. \end{aligned} \tag{3.16}$$

For the entire calculation see Ref. [4]. After the equal sign in Eq. (3.16) the letters $p, q, r,$ and s indicate both hole and particle states, while the letters i and j indicate

hole states. By combining the terms in equations (3.15) and (3.16) we write the entire Hamiltonian as

$$H = \sum_{pq} \langle p|h|q\rangle N(a_p^\dagger a_q) + \sum_i \langle i|h|i\rangle + \frac{1}{2}\sum_{ij} \langle ij|V|ij\rangle + \frac{1}{4}\sum_{pqrs} \langle pq|V|rs\rangle N(a_p^\dagger a_q^\dagger a_s a_r) + \sum_{ipq} \langle pi|V|qi\rangle N(a_p^\dagger a_q), \tag{3.17}$$

where p, q, r, and s still run over all states, i and j over hole states only.

Chapter 4

Perturbation Theory

Perturbation theory[1] is one of the methods used for solving the many-body Schrödinger equation. The starting point usually splits the Hamiltonian in an unperturbed part and a perturbed part. The perturbed part is the one which considers the interactions between the particles. We write the Schrödinger equation as

$$H\Psi = (H_0 + V_I)\Psi = E\Psi, \tag{4.1}$$

where H_0 is the unperturbed Hamiltonian with a known solution. The unperturbed Hamiltonian is a sum of one-particle operators, h_0, which in most of the problems governing nuclear physics is a harmonic oscillator Hamiltonian. The unperturbed part is written as $H_0 = T + U$, where T denotes the kinetic energy of the system and U is the single particle potential. We write the perturbed part as $V_I = V - U$.
Obviously the difference $V - U$ should be small enough so that treating V_I as a perturbation is valid. The exact result is independent of the one particle potential U, but in an approximated calculation it is possible that the results depend on the one-particle potential that is included in the calculations. The eigenfunctions, Φ_i of the unperturbed Hamiltonian are taken as a basis for the expansion of the eigenfunction Ψ,

$$|\Psi\rangle = \sum_{i=1} \alpha_i |\Phi_i\rangle. \tag{4.2}$$

To simplify the calculations it is common practice to divide the space in a model space and an excluded space. By doing this we define two projection operators, that we will meet again later. These projection operators are denoted by a P and a Q. The P operator projects the complete wavefunction onto the model space

$$P|\Psi\rangle = |\Psi_M\rangle, \tag{4.3}$$

[1]This chapter is mainly based on the work in Ref. [10].

while Q is the complimentary projection operator and connects the complete wavefunction with the excluded state $|\Psi_Q\rangle$. They are written as

$$P = \sum_{i=1}^{d} |\Phi_i\rangle\langle\Phi_i| \text{ and } Q = \sum_{i=d+1}^{N} |\Phi_i\rangle\langle\Phi_i| \tag{4.4}$$

The projection operators satisfy the properties

$$P^2 = P,\ Q^2 = Q,\ PQ = QP = 0 \text{ and } P + Q = 1. \tag{4.5}$$

Since $\mathcal{E}_k$ are the eigenvalues of the unperturbed Hamiltonian H_0, we obtain that

$$(E - \mathcal{E}_j)\alpha_j = \langle\Phi_j|V|\Psi\rangle. \tag{4.6}$$

By using this relation we write the entire wavefunction $|\Psi\rangle$ as

$$|\Psi\rangle = \sum_{i=1}^{d} \alpha_i|\Phi_i\rangle + \sum_{i=d+1}^{N} \frac{|\Phi_i\rangle\langle\Phi_i|V|\Psi\rangle}{E - \mathcal{E}_i} = \sum_{i=1}^{d} \alpha_i|\Phi_i\rangle + \frac{QV}{E - H_0}|\Psi\rangle = P|\Psi\rangle + \frac{QV}{E - H_0}|\Psi\rangle.$$

If we now define a wave operator which projects the model space onto the complete wavefunction $\Omega|\Psi_M\rangle = |\Psi\rangle$ we arrive to

$$\Omega(E) = 1 + \frac{Q}{E - H_0} V\Omega(E). \tag{4.7}$$

By using the wave operator in Eq (4.6) we get

$$(E - \mathcal{E}_j)\alpha_j = \langle\Phi_j|V\Omega|\Psi_M\rangle = \sum_{k=1}^{d} \langle\Phi_j|V\Omega|\Phi_k\rangle\alpha_k \tag{4.8}$$

which is equivalent to

$$[H_0 + V\Omega(E) - E]\Psi_M = 0. \tag{4.9}$$

We will define an effective interaction

$$\mathcal{V}(E) = V\Omega(E) \tag{4.10}$$

to get an integral equation,

$$\mathcal{V}(E) = V + V\frac{Q}{E - H_0}\mathcal{V}(\Omega), \tag{4.11}$$

, which is dependent on the energy E. Equation (4.11) can be solved by iteration, where we by using V as a first guess find that

$$\begin{aligned}\mathcal{V}(E) = V + VQ\frac{1}{E-H_0}QV + VQ\frac{1}{E-H_0}QVQ\frac{1}{E-H_0}QV + \\ VQ\frac{1}{E-H_0}QVQ\frac{1}{E-H_0}QVQ\frac{1}{E-H_0}QV + \cdots .\end{aligned} \tag{4.12}$$

This can be solved analytically by observing that the expression above resembles a geometric sum which can be rewritten as

$$\mathcal{V} = V + VQ\frac{1}{E-H_0-QVQ}QV = PVP + PVQ\frac{1}{E-QHQ}QVP. \tag{4.13}$$

4.1 Time dependent perturbation theory

When doing time dependent perturbation theory we have to define a time evolution propagator $U(t,t')$. The time evolution operator evolves a state $\Psi(t')$ at time t' to a state $\Psi(t)$ at time t

$$\Psi(t) = U(t,t')\Psi(t'). \tag{4.14}$$

The wavefunctions satisfy the time dependent Schrödinger equation,

$$\begin{aligned} i\frac{\partial}{\partial t}\Psi(t) &= H\Psi(t) \\ i\frac{\partial}{\partial t}\Psi(t) &= i\frac{\partial}{\partial t}\left[U(t,t')\Psi(t')\right], \end{aligned} \tag{4.15}$$

which yields that the time evolution operator satisfies the time dependent Schrödinger equation. By solving the equation we find the time evolution operator to be

$$U(t,t') = e^{-iH(t-t')}. \tag{4.16}$$

This form of the time evolution operator gives right away the properties one would expect of an operator of this kind. These properties can be summarized as

$$U(t,t) = 1,\ U(t',t)U(t,t') = 1 \tag{4.17}$$

and

$$U(t,t')U(t,t')^\dagger = \ U(t,t')^\dagger U(t,t') = 1, \tag{4.18}$$

From these definitions it follows that the complex conjugate of the time evolution operator is also its inverse and that interchanging t and t' is the same as taking the complex conjugate, see below,

$$U(t',t) = U(t,t')^\dagger = U(t,t')^{-1},\ U(t_1,t_2)U(t_2,t_3) = U(t_1,t_3). \tag{4.19}$$

By use of Gell-Mann's theorem Ref. [11], exact eigenstates can be constructed through the action of the time-development operator. In the present approach the time t will be rotated by a small angle ϵ, thus t is a complex quantity.
We write the eigenstate as

$$\frac{|\Psi_i\rangle}{\langle\Phi|\Psi_i\rangle} = \lim_{\epsilon\to 0} \lim_{t'\to -\infty(1-i\epsilon)} \frac{U(t,t')|\Phi\rangle}{\langle\Phi|U(t,t')|\Phi\rangle}, \tag{4.20}$$

where $|\Psi_i\rangle$ is the lowest state of H with $\langle\Phi|\Psi_i\rangle \neq 0$. This relationship is very useful in calculating the ground state energy shift ΔE_0.

If our unperturbed Hamiltonian gives the energy E_0 while acting on the unperturbed state $|\Phi\rangle$, and our total energy is $E,$ the ground state energy shift is given by

$$\begin{aligned} \Delta E_0 = E - E_0 &= \frac{\langle\Phi|V|\Psi\rangle}{\langle\Phi|\Psi\rangle} \\ &= \lim_{\epsilon\to 0^+} \lim_{t'\to -\infty(1-i\epsilon)} \frac{\langle\Phi|VU(0,t')|\Phi\rangle}{\langle\Phi|U(0,t')|\Phi\rangle}. \end{aligned} \tag{4.21}$$

To evaluate this as a perturbation, we expand the time evolution operator $U(t,t')$. This is most conveniently done in the so-called interaction picture, to be explained below. See also Refs. [12, 13] for more details. The interaction picture can be understood as an intermediate between the Schrödinger picture and the Heisenberg picture. In the Schrödinger picture the operators are time independent while the state evolves with time. It is all contrary in the Heisenberg picture where the operators now are time dependent and the state is time independent. In the interaction picture both the state vectors and the operators are time dependent, however their time dependencies are somehow different.

A state vector in the interaction picture is defined as

$$|\psi_I(t)\rangle = e^{iH_{0,S}t}|\psi_s(t)\rangle, \tag{4.22}$$

where the letter S stands for the Schrödinger picture. Operators in the interaction picture are defined as

$$A_I(t) = e^{iH_{0,S}t}A_S(t)e^{-iH_{0,S}t}, \tag{4.23}$$

where H_0 is the unperturbed Hamiltonian. The time evolution of the operators is given by

$$i\frac{d}{dt}A_I(t) = [A_I(t), H_0]\,. \tag{4.24}$$

By using the definition of one-particle and two-particle operators from chapter 3, our Hamiltonian can be written as in Eq. (3.5), we write it again here as

$$H = \sum_k \epsilon_k a_k^\dagger a_k + \frac{1}{2}\sum_{ijkl} V_{ijkl} a_i^\dagger a_j^\dagger a_l a_k.$$

From Eq. (4.24) we see that it suffices to find the time evolution of the creation and annihilation operators $a^\dagger$ and a to find the time evolution of the Hamiltonian. The commutator between the creation operator and the unperturbed Hamiltonian is

$$\left[a_k^\dagger, H_0\right] = -\epsilon a_k^\dagger(t) \tag{4.25}$$

thus we obtain the time dependence of the creation and destruction operators as

$$a^\dagger(t)_k = a_k^\dagger e^{i\epsilon_k t}$$

and

$$a(t)_k = a_k e^{-i\epsilon_k t}$$

respectively.

We will now transform the Schrödinger equation to the interaction picture

$$\begin{aligned}\psi_I(t) &= e^{iH_0 t}\psi(t) \\ &= e^{iH_0 t}U(t,t')e^{-iH_0 t'}e^{iH_0 t'}\psi(t') \\ &= U_I(t,t')\psi_I(t')\end{aligned} \tag{4.26}$$

By differentiating Eq. (4.26) with respect to time t we find that

$$\frac{\partial}{\partial t}U(t,t') = VU(t,t'). \tag{4.27}$$

When we have found how the time evolution operator behaves with time, we may also find the perturbative expansion of the time evolution operator. The solution to the differential equation is

$$U(t,t') = 1 - i\int_{t'}^{t} dt_1 V(t_1)U(t_1,t') \tag{4.28}$$

Equation (4.28) can be solved by iteration using

$$U(t,t') = 1 + \sum_{n=1}^{\infty}(-i)^n \int_{t'}^{t} dt_1 \int_{t'}^{t_1} dt_2 \cdots \int_{t'}^{t_{n-1}} dt_n V(t_1)V(t_2)\cdots V(t_n). \tag{4.29}$$

4.2 Feynman-Goldstone diagrams

To evaluate Eq. (4.20) we had to define a new operator, called the time ordering operator. The effect of the time ordering operator on a product of operators is to order the them so the operators with a larger time argument are placed to the left to those of smaller time arguments. Since we in nuclear physics are dealing with fermions which obey the Pauli exclusion principle there will be a sign dependency on the number of permutations needed in making the arrangement. As an example

$$\begin{aligned} &T\left[A_1(t_1)A_2(t_2)\cdots A_n(t_n)\right] \\ &= (-1)^p A_\alpha(t_\alpha)A_\beta(t_\beta)\cdots A_\gamma(t_\gamma) \end{aligned} \tag{4.30}$$

If we use time ordering together with the particle hole formalism from section 3.3, we will find a new definition of the contraction. A contraction of two operators will now be defined as

$$\overbrace{AB} = T[AB] - N[AB], \tag{4.31}$$

where $N[AB]$ is the normal ordering operator. As an example we will derive a contraction of two hole operators and a contraction of two particle operators. We will first start with a contraction of two hole operators where both particles have momenta below k_F, and with $t < t'$.

$$\begin{aligned} \overbrace{a_h(t)a^\dagger_{h'}}(t') &= T\left[a_h(t)a^\dagger_{h'}(t')\right] - N\left[a_h(t)a^\dagger_{h'}(t')\right] \\ &= -a^\dagger_{h'}(t')a_h(t) - a_h(t)a^\dagger_{h'}(t') \\ &= -\left(a^\dagger_{h'}(t')a_h(t) + a_h(t)a^\dagger_{h'}(t')\right)e^{-i(\epsilon_h t - \epsilon_{h'}t')} \\ &= -\delta_{h,h'}e^{-i(\epsilon_h t - \epsilon_{h'}t')}. \end{aligned} \tag{4.32}$$

Similarly for particles with momenta above k_F and $t < t'$

$$\overbrace{a_p(t)a_{p'}}(t') = \delta_{p,p'}e^{-i\epsilon_p(t-t')} \tag{4.33}$$

We have

$$\overbrace{a_\alpha(t)a^\dagger_\beta}(t') = -\overbrace{a^\dagger_\beta(t')a_\alpha}(t) \tag{4.34}$$

In Fig (4.1) the two contractions in Eqs (4.32) and (4.33) are represented diagrammatically, the annihilation operator a_α destroys the particle line $a^\dagger_\beta$ creates. The time is upward.

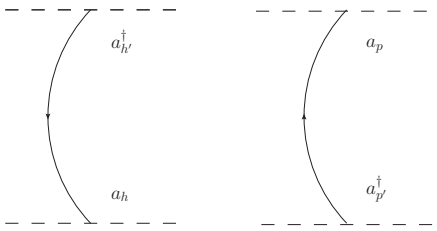

Figure 4.1: Diagrammatic representation of the contractions in Eqs. (4.32) and (4.33) The time is going upward.

With the above definitions of time ordering and contractions we are ready to go back to the time evolution operator, which is already in a time ordered form

$$U(t,t') = \sum_{n=0}^{\infty} (-i)^n \int_{t'}^{t} dt_1 \int_{t'}^{t_1} dt_2 \cdots \int_{t'}^{t_{n-1}} dt_n T\left[V(t_1)V(t_2)\cdots V(t_n)\right]. \quad (4.35)$$

From Eq. (4.35) we see that there are $n!$ ways to order the multidimensional integral with respect to the times $t_1, t_2 \cdots t_n$, it is again possible to rewrite the time evolution operator to the form

$$U(t,t') = \sum_{n=0}^{\infty} \frac{1}{n!} (-i)^n \int_{t'}^{t} dt_1 \int_{t'}^{t} dt_2 \cdots \int_{t'}^{t} dt_n T\left[V(t_1)V(t_2)\cdots V(t_n)\right] \quad (4.36)$$

If we recall that it is the energy shift we want to calculate, we can use the above equation to write the numerator and the denominator in Eq. (4.21) as

$$\sum_{n=0}^{\infty} \frac{1}{n!} (-i)^n \int_{t'}^{t} dt_1 \int_{t'}^{t} dt_2 \cdots \int_{t'}^{t} dt_n \langle\phi| T\left[V(t)V(t_1)V(t_2)\cdots V(t_n)\right] |\phi\rangle \quad (4.37)$$

and

$$\sum_{n=0}^{\infty} \frac{1}{n!} (-i)^n \int_{t'}^{t} dt_1 \int_{t'}^{t} dt_2 \cdots \int_{t'}^{t} dt_n \langle\phi| T\left[V(t_1)V(t_2)\cdots V(t_n)\right] |\phi\rangle \quad (4.38)$$

respectively. To evaluate the integrals in the numerator and the denominator we have to use Wick's theorem, Wick's theorem with time ordering will be slightly modified from the first version in section 3.2. Wicks theorem states now that

$$\begin{aligned} T\left[A(t_1)B(t_2)C(t_3)\cdots Z(t_n)\right] &= N\left[A(t_1)B(t_2)C(T_3)\cdots Z(t_n)\right] \\ &+ \sum_{1\,contraction} N\left[A(t_1)B(t_2)C(T_3)\cdots Z(t_n)\right] + \sum_{2\,contractions} N\left[A(t_1)B(t_2)C(T_3)\cdots Z(t_n)\right] \\ &+ \cdots + \sum_{\substack{contractions\,with\\ all\,operators}} N\left[A(t_1)B(t_2)C(T_3)\cdots Z(t_n)\right]. \end{aligned} \quad (4.39)$$

Since our unperturbed state is the groundstate, our reference vacuum state, only the last term in Eq. (4.39) survives. Further all unlinked diagrams in the numerator, ie. all contractions which does not include the interaction $V(t)$ are canceled by the diagrams in the denominator.

Let us now evaluate the first-order contribution to the energy shift in Eq. (4.21). The only contributing term is $V(t)$ which on a second quantized form is written as $v_{\alpha\beta\gamma\delta}a^\dagger_\alpha(t)a^\dagger_\beta(t)a_\delta(t)a_\gamma(t)$. From Wick's theorem we will then have two terms contributing to the energy shift.

$$\overbrace{a^\dagger_\alpha(t)\overbrace{a^\dagger_\beta(t)a_\delta(t)}a_\gamma(t)} + \overbrace{a^\dagger_\alpha(t)\overbrace{a^\dagger_\beta(t)a_\delta(t)a_\gamma(t)}} \tag{4.40}$$

The terms in Eq. (4.40) can be depicted diagrammatically as seen in Fig 4.2. The

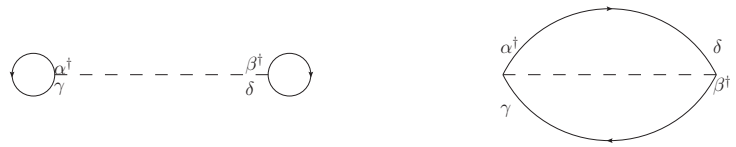

Figure 4.2: Diagrammatic representation of the first order diagram, the diagram to the left depicts the first term in Eq. (4.40), the diagram to the right depicts the second term in Eq. (4.40).

single particle states α, β, γ and δ must all be holes, since they are all equal time operators. The energy shift can now be written as

$$\Delta E_0 = \frac{1}{2}\sum_{\alpha\beta<k_f}\frac{1}{2}(v_{\alpha\beta\alpha\beta} - v_{\alpha\beta\beta\alpha}), \tag{4.41}$$

the minus sign comes in, by the "rule" that for every contraction that crosses another one, contributes with a factor (-1).

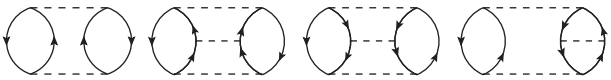

Figure 4.3: Diagrammatic representation of second to third order contribution to the energy.

Fig 4.3 depicts second- and third-order contributions to the energy, with the rules for computing the diagrams the second order contribution is

$$\Delta E^{(2)} = \frac{\langle ij|V|ab\rangle\langle ab|V|ij\rangle}{\epsilon_{ij} - \epsilon_{ab}}, \tag{4.42}$$

where $\epsilon_{pq} = \epsilon_p + \epsilon_q$, denotes the single particle energies and the indexes i and j runs over states occupied in the reference vacuum and a and b runs over single-particle states not occupied in the reference vacuum.

With the clever invention of diagrams that depict the contractions, we are able to describe every term in the expansion of the time evolution operator as diagrams. These diagrams are usually called Feynman diagrams or Feynman-Goldstone diagrams, to honor the inventors. When presenting all the terms as diagrams we need some rules to keep track of them. The idea is that we find a term in the expansion by studying the corresponding diagram. A nice derivation of the diagram rules can be found in Ref. [14]. The rules are summarized in appendix A.

Chapter 5

Nuclear matter

Nuclear matter is an idealized theoretical system of nucleons, it can be thought of as a nucleus composed of infinitely many nucleons. This chapter will review some of the properties of nuclei. It is unfortunately impossible to cover all the physics concerning nuclear physics, and the author humbly has to admit that much of it is still unclear. We will first go through the nuclear forces and nuclear structure before we finish the chapter with the shell model.

5.1 Nuclear structure

The binding energy, $B(N,Z)$, is given by

$$B(N,Z) = \big(Nm_n + Zm_p - M(N,Z)\big), \tag{5.1}$$

where N is the neutron number and Z is the proton number. The binding energy is almost proportional to the number of particles (both protons and neutrons), A, composing the nucleus, see Ref.[15].
It is also found by experiments that the radius, R, of a nucleus increases with the number of particles, $R = r_0 A^{1/3}$. The value of r_0 is estimated by experiments to be approximately 1.2 fm, see for example [16]. When the nucleus is considered to be spherical, the volume, $\Omega = 4\pi R^3/3$, is linearly dependent on the number of particles, as a consequence the particle density in a nucleus is independent of the number of constituents. By dividing the volume by the number of constituents in a nucleus results in a particle density on the form

$$\frac{A}{\Omega} = \frac{3}{4\pi r_0^3} \approx 1.95 \times 10^{38}\,\text{particles/cm}^3 \tag{5.2}$$

Since the volume of a nucleus depends linearly on the number of particles (as a

droplet does), we can model the nucleus with a liquid drop. With the liquid drop model we are able to find a formula for the mass of a nucleus. Since this formula is obtained with both empirical data and theoretical assumptions this formula is called the semi-empirical mass formula. The binding energy has (by using scattering data on nucleon-nucleon interaction) been parametrized as

$$B = a_v A - a_S A^{2/3} - a_C \frac{Z(Z-1)}{A^{1/3}} - a_A \frac{(A-2Z)^2}{A} + \delta(A,Z). \tag{5.3}$$

The first term is called the volume term, this term satisfy the almost linearly dependence on the nucleon number A. This linearly dependence of A indicates that each nucleon attracts only it closest neighbors and not all the other nucleons. Since we from experiments, such as electron scattering, have concluded that the nucleus density is constant, every nucleon has the same amount of closest neighbors. The exception are those nucleons that lie on the surface of the nucleus, thus we have to subtract this term, since the term $a_v A$ is an overestimate. The surface nucleons contribute with a negative term $-a_s A^{2/3}$. The repulsive coulomb term of the protons should also be taken into consideration, assuming a uniformly charged sphere, we obtain that the contribution is

$$-a_C \frac{Z(Z-1)}{A^{1/3}}.$$

There are two more terms left, which are mainly extracted from experiments. The first one is called the asymmetry term, it accounts for the effect that the most stable nuclei are symmetric, we include the term

$$-a_A \frac{(A-2Z)^2}{A}.$$

The last term is the pairing term, which accounts for the fact that the most stable configuration is when the number of nucleons of the same kind with spin up is equal to the number of nucleons with spin down, which is a property because of the Pauli principle. The pairing term does not contribute if we have an odd number of nucleons, but affect the mass or binding energy differently in the two cases of even-even nuclei and odd-odd nuclei, we give it the symbol $\delta(A,Z)$, its contribution to the formula is

$$\delta(A,Z) = \begin{cases} +\delta_0 & Z, N \text{ even } (A \text{ even}) \\ 0 & A \text{ odd} \\ -\delta_0 & Z, N \text{ odd } (A \text{ even}) \end{cases}$$

To find the mass of a given nucleus we subtract the binding energy from the sum of the nucleon masses as done here;

$$m = Z m_p + N m_n - \frac{B}{c^2}. \tag{5.4}$$

5.2 A review of nuclear forces

The mere existence of the deuteron is an evidence of the nuclear force, or the strong force, and that the force between protons and neutrons have to be attractive at least in the $J^\pi = 1^+$ state, or the ${}^3S_1$ partial wave state, which carries the quantum numbers of the deuteron.

Interference between Coulomb and nuclear scattering for the proton-proton partial wave ${}^1S_0$ shows that the nucleon-nucleon force is attractive at least for the ${}^1S_0$ partial wave, and that it has to be greater than the coulomb force at small distances. If not the protons would have been repelled by the repulsive electromagnetic forces the protons mediates with each other. However for interparticle distances of atomic scale, the nucleon-nucleon interaction (of the strong force) is negligible. The cross section for neutron-proton scattering is isotropic for energies up to 10 MeV in the center of mass frame, it is then concluded that the scattering occurs in the relative S states.

The nuclear force is the same as the strong force, the one of quarks and gluons. The same force that holds the nucleus together is the same that keeps together the quarks that combine to make up hadrons. Hadrons are particles that feel the strong force and are composite of quarks. The nucleons consist of the up, u and down, d quarks. There are three generations of quarks, six quarks in total. Beside the already mentioned u and d quarks, we have the charm quark, c, strange quark s, the top quark t and the bottom quark b. They were not all discovered at the same time, the most heavy, the top quark was not discovered until 1995 by the CDF and D0 experiments at Fermilab, [17, 18]. We state the three generations of quarks as

$$\begin{pmatrix} u \\ d \end{pmatrix}, \begin{pmatrix} c \\ s \end{pmatrix} \text{ and } \begin{pmatrix} t \\ b \end{pmatrix}. \tag{5.5}$$

All quarks have both electric charge and color charge. The electric charges differ by e in each generation, where the upper ones have $2/3e$ and the lower have charges $-1/3e$, where e is the electron charge. There are three types of color charges red, blue and green. The quarks are spin half particles which have to obey the Pauli principle.

The nucleons, the proton and neutron, consist of three quarks. The proton consists of two u quarks and one d quark which combine to the electric charge of one e. The neutron consists of two d quarks and one u quark which make the neutron electrically neutral.

Much of what is known about nucleons is by combinations of experiment and theoretical predictions. Much is known by nucleon-nucleon scattering. By calculating the differential cross section for nucleon-nucleon scattering it is understood that the nuclear potential depends not only on the coordinates, but also on the spin of the particles. The definition of the differential cross section $d\sigma/d\Omega$, is the probability per unit solid angle that an incident particle is scattered into the solid angle $d\Omega$. The standard unit for measuring a cross section is the barn, b, and it is equal to $10^{-28}\mathrm{m}^2$. The probability $d\sigma$ that an incident particle is scattered into $d\Omega$ is the ratio of the scattered current through $d\Omega$ to the incident current, see Ref. [16]

$$d\sigma = \frac{(j_{scattered})r^2 d\Omega}{j_{incident}} \tag{5.6}$$

If we use that the current of the particles is

$$\mathbf{j} = \frac{1}{2mi}(\psi^*\nabla\psi - (\nabla\psi^*)\psi), \tag{5.7}$$

which is found by multiplying the Schrödinger equation with ψ^*,

$$i\psi^*\frac{\partial\psi}{\partial t} + \frac{1}{2m}\psi^*\nabla^2\psi = i\frac{\partial}{\partial t}(\psi^*\psi) - i\frac{\partial\psi^*}{\partial t}\psi + \frac{1}{2m}\psi^*\psi$$
$$= i\frac{\partial}{\partial t}(\psi^*\psi) + \frac{1}{2m}\nabla\left(\psi^*\nabla\psi - (\nabla\psi^*)\psi\right) = 0 \Rightarrow \frac{\partial\rho}{\partial t} + \nabla\cdot\mathbf{j} = 0,$$

where $\rho = \psi^*\psi$ is interpreted as the probability density.
It is just a matter of finding the wave function to calculate the cross section. We let the incoming wave have the form

$$\psi_{incident} = \frac{A}{2ik}\left[\frac{e^{ikr}}{r} - \frac{e^{-ikr}}{r}\right]. \tag{5.8}$$

This form keeps the incident wave finite as $r \to 0$. By assuming that the scattering cannot create or destroy particles, but only change the phase of the outgoing wave, the total wavefunction can be written as

$$\psi(r) = \frac{A}{2i}e^{-i\delta}\left[\frac{e^{i(kr+i2\delta)}}{r} - \frac{e^{-ikr}}{r}\right]. \tag{5.9}$$

To find the scattered wave function we subtract the incident wave function Eq. (5.8) from Eq. (5.9), where δ is the phase shift. The nodes of the wave function will be pushed away from the potential it sees if the phase shift is negative and pulled inwards if the phase shift is positive.

By using the formula for the differential cross section, Eq. (5.6), we find it to be

$$\frac{d\sigma}{d\Omega} = \frac{sin^2(\delta)}{k^2}. \tag{5.10}$$

The total cross section, which is interpreted as the probability to be scattered in any direction is in the special case for $l = 0$

$$\sigma = \frac{4\pi sin^2(\delta)}{k^2}. \tag{5.11}$$

In order to get a better estimate to the cross section we need to consider the spins. Nucleons are fermions with spin 1/2 and in the scattering process they combine to either total spin 1, the triplet state or total spin 0, the singlet state. The total cross section should then be the sum of the cross sections for all of the possible states they can be in. There are in total four possible spin states, three spin 1 states and one spin 0 state. The probability for being in one of the triplet states is 3/4 and in the singlet state 1/4. We can now write down the total cross section as

$$\sigma = \frac{3}{4}\sigma_t + \frac{1}{4}\sigma_s, \tag{5.12}$$

where σ_t indicates the cross section for spin 1 states, and σ_s for the spin 0 state. By using parameters from deuteron scattering it is found that there is a significant difference between the cross sections for the triplet state and singlet state, $\sigma_t = 4.6$ b and $\sigma_s = 67.8$ b. This difference can only be explained by a spin dependency in the nuclear force.

If we assume that the charge is invariant under charge symmetry breaking and isospin symmetry breaking then the different nucleon-nucleon interaction channels, the proton-proton, neutron-neutron and neutron-proton, are all identical. However in reality this symmetry is broken.

Observations that the ground state of the deuteron is a mixed state of orbital momentum $l = 2$ and $l = 0$ indicate that the nucleon-nucleon potential cannot be invariant under spatial rotations alone. The most general velocity-independent potential that is invariant under overall roations reflection is on the form $V_T(r)S_{12}$

$$S_{12} = 3(\sigma_1 \cdot \mathbf{r})(\sigma_2 \cdot \mathbf{r})/r^2 - \sigma_1 \cdot \sigma_2. \tag{5.13}$$

This term gives rise to the tensor force. There is also a non-local part remaining, the so-called spin orbit term $V_{LS} = V_{LS}(r)\mathbf{L} \cdot \mathbf{S}$.

5.3 The shell model

The shell model description of the nucleus is in some senses similar to the description of atomic shell structures. It is actually the atomic shell model that is the starting point since it has been so effective in describing the atoms. Nuclear physicists attempted to describe nuclear theory in a similar way.

There are however several important differences. In the atomic case the electrons are orbiting the nucleus which acts as an external potential. In the nucleus there is no external potential, the nucleons make their own field. In the atomic case there is just one sort of particles to solve for, the electrons, at least in the Born-Oppenheimer approximation. In the nuclear case we have two types of particles, protons and neutrons. Evidence of a shell structure is increased stability of the nuclei when they have a certain number Z of protons and N of neutrons. We call these nuclei for magic nuclei. Magic nuclei are determined to have Z or $N = 2,\ 8,\ 20,\ 28,\ 50,\ 82,\ 126$. These numbers are more or less explained by introducing a one-body attractive average field in the Hamiltonian,

$$H = T + V(r_1, r_2) = H = T + U(r) + V(r_1, r_2) - U(r) = T + U + V_I$$
$$= H_0 + V_I$$

here H_0 denotes an attractive, or bounded one-body potential all nucleons feel. The smaller V_I is, the better is the assumption of an independent field.

The question that arises is what form the potential should have, to give the correct magic nuclei. In Ref. [16] they are using a potential on an intermediate form between an infinite well and a harmonic potential

$$U(r) = \frac{-U_0}{1 + e^{\frac{r-R}{a}}},$$

where R is the mean nuclear radius and a is the skin thickness. The skin thickness is related to the charge density of a nucleus. It is the distance onver which the charge density falls from 90% of its central value to 10%. The skin thickness value a is approximately 2.3 fm. However in order to get all the magic numbers they had to add a spin orbit term to the potential, a factor $U_{sl} l \cdot s$. By using the angular momentum relations

$$j^2 = (l + s)^2 = l^2 + s^2 + 2l \cdot s$$
$$l \cdot s = \frac{1}{2}(j^2 - l^2 - s^2)$$

and inserting for the eigenvalues for j, l and s we find the factor to be

$$\langle l \cdot s \rangle = \frac{1}{2}\left(j(j+1) + l(l+1) + \frac{3}{4}\right).$$

With the additional ls term one could explain the magic numbers.

5.4 Energy per particle

The main goal of physics is understanding the world and forces surrounding us, when we have a model we need it to predict some properties which we can measure, such as the force or the energy. In the case of nuclear matter it is the energy per particle which is the quantity we wish to compare with the experimentally known value. This quantity is called the binding energy. By dividing the binding energy with the nucleon number A,

$$B = \frac{E}{A} = \frac{E_{kin}}{A} + \frac{E_{interaction}}{A}. \tag{5.14}$$

we can find an "experimental" value of the binding energy per nucleon for symmetric nuclear matter, i.e., when the nucleon number goes to infinity, with an equal amount of protons and neutrons. From Eq. (5.3) we see that the only surviving term is the volume term a_v which is approximately 16 MeV.

As physicists we are not satisfied with just empirical and experimental values. We want to understand why it is so. We want to derive it with the theoretical tools available, but this task is a formidable one.

If we approximate the wave functions as plane waves and assume that the nucleons form a non-interacting Fermi gas, we can estimate the saturation density which corresponds to the Fermi momentum k_f.
The number of particles in a non-interacting Fermi gas is given by the equation

$$N = \nu \int_0^{k_f} \Omega \frac{d^3k}{(2\pi)^3} = \Omega\nu \frac{k_f^3}{3 \cdot 2\pi^2}, \tag{5.15}$$

where ν is the degeneracy factor and Ω indicates the volume. The degeneracy factor ν is in the nuclear case equal to four. We have two isospin states and two spin states. From the quantum mechanical solution to the infinite well, with sides L, we can show that the principal number n is related to the wave number k by

$$k = \frac{2\pi n}{L}. \tag{5.16}$$

When we operate in a three dimensional world $d^3n = d^3kL^3/(2\pi)^3$ where $L^3 = \Omega$. Since we let the volume go to infinity the amount of particles gets undefined, however the particle density is a well defined quantity by dividing Eq. (5.15) by Ω and

performing the integral over k we get the density

$$\rho = \nu \frac{k_f^3}{3 \cdot 2\pi^2}. \tag{5.17}$$

With these relations it is possible to calculate the Fermi level of nuclear matter, in section (5.3) we found a value for

$$\frac{A}{\Omega} = \frac{2k_f^3}{3 \cdot \pi^2} = 1.95 \times 10^{38}.$$

Here we have used that the degeneracy factor ν is equal to four, we find that the Fermi level corresponds to $k_f \approx 1.42$ fm^{-1}.
The kinetic energy density is calculated by the formula

$$\int_0^{k_f} dk \frac{3k^4}{4mk_f^3} = \frac{3k_f^2}{2 \cdot 5m}. \tag{5.18}$$

The interaction part is at least a two-body interaction. It is convenient to work in the momentum picture and we write our two-body interaction as

$$\begin{aligned} &\sum_{\substack{j_a l_a, tz_a, j_b, l_b, tz_b \\ j_c, l_c, tz_c, j_d, l_d, tz_d}} \int \frac{d^3k_a}{(2\pi)^3} \int \frac{d^3k_b}{(2\pi)^3} \int \frac{d^3k_c}{(2\pi)^3} \int \frac{d^3k_d}{(2\pi)^3} \\ &\times \langle k_a j_a l_a tz_a k_b j_b l_b tz_b JTz | V(k_a, k_b, k_c, k_d) | k_c j_c l_c tz_c k_d j_d l_d tz_d JTz \rangle \end{aligned} \tag{5.19}$$

In section 8.2 we show how this is computed in the space of relative and center of mass coordinates. The form of the potential may be the Bonn potential or N^{3}LO used in our project.

Chapter 6

The nucleon-nucleon potential

Since Chadwick discovered the neutron in 1932, understanding the nucleon-nucleon interaction has been a main focus for nuclear physicists. Yukawa proposed the first significant theory of the nuclear force, see Ref. [19], where a meson is exchanged in the nucleon-nucleon interaction. This meson was later to be identified with the pion. The one-pion-exchange model turned out to be very useful in explaining data on nucleon-nucleon scattering and the properties of the deuteron, see for example Ref. [20]. Problems arose when multipion exchange were included, and the "pion theories" of the 1950's are generally judged to be failures, see for example Ref. [20]. The reasons for the failure of the theories in the fifties is because of the then unknown pion dynamics understood by Quantum chromodynamics (QCD) and chiral symmetries, which were not to be used by the nuclear physicists until the eighties.

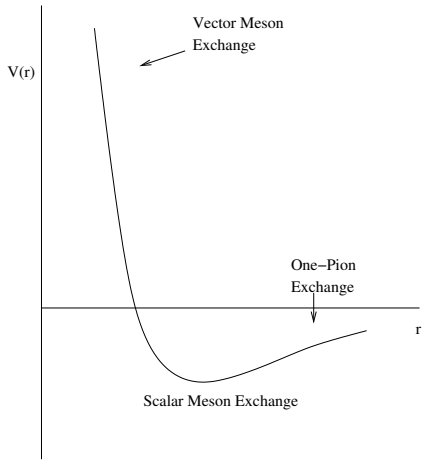

Figure 6.1: Schematic plot of the nucleon-nucleon interaction.

6.1 Chiral Perturbation Theory

The discovery of QCD and the understanding of effective field theory was a breakthrough for understanding the nucleon-nucleon potential.
QCD is the theory of the strong interaction, where quarks and gluons are treated as the degrees of freedom. The principles behind the theory are really simple and elegant, the interactions are derived by demanding that the Lagrangian is gauge invariant under SU(3) group transformations.
QCD is a non-Abelian field theory as a consequence of the discovery of the three quantum numbers of color, where the underlying gauge group is the SU(3) group. QCD is well-known for the word ”Asymptotic freedom”. With ”asymptotic freedom” we say that the force governing QCD is weak at short distances but strong, at long distances or at low energies. The consequences it brings us is that QCD is perturbative at high energies, but non-perturbative at low, and that the quarks and gluons are confined into ”colorless” objects, called hadrons. The non-perturbativity of QCD at the low energy regime is problematic, the coupling constants are too huge, it becomes meaningless to do a perturbative approach since we end up with divergencies at every order of the expansion parameter. As noted earlier, in nuclear physics we operate in this limit, and difficulties arise when treating quarks and gluons in the nuclear force. The solution is to identify the relevant degrees of freedom, which in the nuclear case are the nucleons and integrate out the irrelevant ones. We treat the nucleons as ”elementary” particles and not as composite of quarks.

When we do this approximation and construct an effective field theory based on QCD, the symmetries of the original Lagrangian must be manifest in the effective Lagrangian. In the case of QCD, the Lagrangian is invariant under SU(3) transformations, which also should be a symmetry of the effective Lagrangian.

In the limit where the quark masses are zero, the so-called chiral limit, the Lagrangian,

$$\mathcal{L} = \bar{q} i\gamma^\mu D_\mu q - \frac{1}{4} G^a_{\mu\nu} G^{\mu\nu,a},$$

may be separated into a Lagrangian of left, q_L, and right handed, q_R, quark fields,

$$\bar{q}_R i\gamma^\mu D_\mu q_R + \bar{q}_L i\gamma^\mu D_\mu q_L - \frac{1}{4} G^a_{\mu\nu} G^{\mu\nu,a},$$

where

$$q_L = \frac{1}{2}(1-\gamma_5)q = P_L q \text{ and } q_R = \frac{1}{2}(1+\gamma_5)q = P_R q.$$

The chirality matrix $\gamma_5 = \gamma^5 = i\gamma^0\gamma^1\gamma^2\gamma^3$, with the properties

$$\{\gamma^\mu, \gamma^5\} = 0 \text{ and } \gamma_5^2 = 0,$$

makes the projection operators P_L and P_R satisfy the properties

$$P_R^2 = P_R,\ P_L^2 = P_L,$$

and the orthogonality relations

$$P_R P_L = P_L P_R = 0,$$

with the completeness relation

$$P_R + P_L = 1.$$

The γ^μ matrices are defined as

$$\gamma^0 = \begin{pmatrix} I & 0 \\ 0 & -I \end{pmatrix} \text{ and } \gamma^i = \begin{pmatrix} 0 & \sigma^i \\ -\sigma^i & 0 \end{pmatrix},$$

where I is the identity matrix and σ the Pauli spin matrices. The ordinary derivative ∂_μ is replaced with the covariant derivative

$$D_\mu = \partial_\mu - ig \sum_{a=1}^{8} \frac{\lambda_a^C}{2} \mathcal{A}_{\mu,a},$$

when we demand invariance under local SU(3) transformations. The SU(3) group transforms by the set eight parameters θ according to

$$q \to q' = e^{-i \sum_{a=1}^{8} \Theta_a(x) \frac{\lambda_a^C}{2}} q = U[g(x)]q,$$

where the so-called Gell-Mann matrices λ^a are given by

$$\lambda^1 = \begin{pmatrix} 0 & 1 & 0 \\ 1 & 0 & 0 \\ 0 & 0 & 0 \end{pmatrix},\ \lambda^2 = \begin{pmatrix} 0 & -i & 0 \\ i & 0 & 0 \\ 0 & 0 & 0 \end{pmatrix},\ \lambda^3 = \begin{pmatrix} 1 & 0 & 0 \\ 0 & -1 & 0 \\ 0 & 0 & 0 \end{pmatrix},$$

$$\lambda^4 = \begin{pmatrix} 0 & 0 & 1 \\ 0 & 0 & 0 \\ 1 & 0 & 0 \end{pmatrix},\ \lambda^5 = \begin{pmatrix} 0 & 0 & -i \\ 0 & 0 & 0 \\ i & 0 & 0 \end{pmatrix},\ \lambda^6 = \begin{pmatrix} 0 & 0 & 0 \\ 0 & 0 & 1 \\ 0 & 1 & 0 \end{pmatrix},$$

$$\lambda^7 = \begin{pmatrix} 0 & 0 & 0 \\ 0 & 0 & -i \\ 0 & i & 0 \end{pmatrix},\ \lambda^8 = \sqrt{\frac{1}{3}} \begin{pmatrix} 1 & 0 & 0 \\ 0 & 1 & 0 \\ 0 & 0 & -2 \end{pmatrix}.$$

The symbol G denotes the gluon field tensor and $\mathcal{A}_{\mu,a}$ denotes the eight independent gauge potentials.
By doing separate left and right handed SU(3) transformations

$$q_L \to q_L' = U_L q_L = e^{-i \sum_{a=1}^{8} \Theta_a^L \frac{\lambda_a}{2}} q_L,$$

$$q_R \rightarrow q'_R = U_R q_R = e^{-i\sum_{a=1}^{8}\Theta_a^R\frac{\lambda_a}{2}} q_R,$$

we will see that the Lagrangian remains unchanged and therefore is invariant under this transformation,

$$\mathcal{L} \rightarrow \mathcal{L}' = \bar{q}_R U_R^\dagger U_R i\gamma^\mu D_\mu q_R + \bar{q}_L U_L^\dagger U_L i\gamma^\mu D_\mu q_L - \frac{1}{4}G^a_{\mu\nu}G^{\mu\nu,a} =$$
$$\bar{q}_R i\gamma^\mu D_\mu q_R + \bar{q}_L i\gamma^\mu D_\mu q_L - \frac{1}{4}G^a_{\mu\nu}G^{\mu\nu,a} = \mathcal{L}.$$

The quarks have a finite mass, but it is not a bad approximation to make them massless in the nuclear scale since $m_{u,d,s} \ll m_N$, where u, d, s denotes the up, down and the strange quark, while m_N stands for the nucleon mass. We will in this chapter only consider the u, d and s quarks.
The remarkable theorem by Emma Noether states that for each symmetry of the Lagrangian there exists a conserved current. Let the Lagrangian $\mathcal{L}(\Phi, \partial_\mu\Phi)$ be invariant under the transformation

$$\Phi \rightarrow \Phi + \alpha\delta\Phi,$$

where α is a small parameter.
This transformation yields a shift in the Lagrangian,

$$\alpha\delta\mathcal{L} = \frac{\partial\mathcal{L}}{\partial\Phi}\alpha\delta\Phi + \frac{\partial\mathcal{L}}{\partial(\partial_\mu\Phi)}\alpha\delta(\partial_\mu\Phi)$$
$$= \alpha\Big(\frac{\partial\mathcal{L}}{\partial\Phi}\delta\Phi - \partial_\mu\frac{\partial\mathcal{L}}{\partial(\partial_\mu\Phi)}\delta\Phi\Big) + \alpha\partial_\mu\Big(\frac{\partial\mathcal{L}}{\partial(\partial_\mu\Phi)}\Big)\delta\Phi = \alpha\partial_\mu\big(\frac{\partial\mathcal{L}}{\partial(\partial_\mu\Phi)}\delta\Phi\big), \quad (6.1)$$

where we have here made use of the equation of motion

$$\Big(\frac{\partial\mathcal{L}}{\partial\Phi} - \partial_\mu\frac{\partial\mathcal{L}}{\partial(\partial_\mu\Phi)}\Big) = 0.$$

When the Lagrangian is invariant under this shift

$$\alpha\delta\mathcal{L} = 0 = \alpha\partial_\mu\big(\frac{\partial\mathcal{L}}{\partial(\partial_\mu\Phi)}\delta\Phi\big) = \alpha\partial_\mu J^\mu, \quad (6.2)$$

we have a conserved current J^μ. In the case of chiral invariance the shift in the fields are

$$-i\Theta_a^L\frac{\lambda^a}{2}q_L$$

for the left-handed quark fields and

$$-i\Theta_a^R\frac{\lambda^a}{2}q_R$$

for the right-handed fields. We have neglected terms of order Θ_L^2 and Θ_R^2 and higher. The eight conserved left-handed currents are

$$L^{\mu,b} = \bar{q}_L \gamma^\mu \frac{\lambda^b}{2} q_L,$$

and the eight conserved right-handed currents are

$$R^{\mu,b} = \bar{q}_R \gamma^\mu \frac{\lambda^b}{2} q_R.$$

However, these currents can combine to a set of vector currents $J_V^{\mu,b}$ and a set of axial currents $J_A^{\mu,b}$, where

$$J_V^{\mu,b} = R^{\mu,b} + L^{\mu,b} = \overline{q} \gamma^\mu \frac{\lambda^b}{2} q \tag{6.3}$$

and

$$J_A^{\mu,b} = R^{\mu,b} - L^{\mu,b} = \overline{q} \gamma^\mu \gamma_5 \frac{\lambda^b}{2} q. \tag{6.4}$$

For each current there is a corresponding conserved charge, Q, which is a generator of $SU(3)_V \times SU(3)_A$. The conserved charges will in this case be

$$Q_V^b = \int d^3x J^{0,b}$$

and

$$Q_A^b = \int d^3x J_A^{0,b}.$$

If a mass term,

$$M = \begin{pmatrix} m_u & 0 & 0 \\ 0 & m_d & 0 \\ 0 & 0 & m_s \end{pmatrix},$$

for the quarks is included in the Lagrangian, the symmetry will break down. Let us look at the QCD Lagrangian with quark masses inserted,

$$\mathcal{L}_{QCD} = \overline{q}(i\gamma^\mu D_\mu - M)q - \frac{1}{4} G^a_{\mu\nu} G^{\mu\nu,a}. \tag{6.5}$$

The mass term mixes the left- and right-handed quark fields

$$\bar{q} M q = \bar{q}_L M q_R + \bar{q}_R M q_L.$$

By introducing explicitly the symmetry breaking mass term, the Lagrangian is no longer invariant under left- and right-handed SU(3) transformations,

$$\bar{q}_L M q_r + \bar{q}_R M q_L \rightarrow \bar{q}_L U_L^\dagger U_R M q_R + \bar{q}_R U_R^\dagger U_L M q_L \neq \bar{q}_L M q_r + \bar{q}_R M q_L,$$

thus the vector and axial currents are in general not conserved, their divergencies satisfy

$$\begin{aligned} \partial_\mu J_V^{\mu,a} &= i\overline{q}[M, \frac{\lambda^a}{2}]q \\ \partial_\mu J_A^{\mu,a} &= i\overline{q}\{\frac{\lambda^a}{2}, M\}\gamma_5 q. \end{aligned} \tag{6.6}$$

For equal quark masses, the vector currents are conserved since all matrices commute with a multiple of the identity matrix. The axial currents are not conserved. The symmetry breaks down to $SU(3)_V$, in the case where the quarks have equal mass.

If a symmetry is spontaneously broken, the ground state is no longer invariant under a certain symmetry, the theory will be enriched by new particles, called Goldstone bosons. These particles will be massless and have the same quantum numbers as the generators that break the symmetry, see for example Ref. [21].
There are reasons to believe that the ground state is not annihilated by the generators of the axial symmetry. If there were an exact axial symmetry we would expect the existence of a degenerate hadron multiplet of opposite parity, see for instance Ref.[22]. For each hadron there should exist a hadron of opposite parity. These multiplets are not observed, so we assume that the axial symmetry is spontaneously broken and expect eight massless Goldstone bosons. The $SU(3)_V$ is still a valid symmetry when the quarks have equal masses.
The involvement of massless Goldstone bosons is problematic, the standard model doesn't account for any extra massless particles. This dilemma is solved by using the fact that the quarks are not massless, this implies that the Goldstone bosons acquire a small effective mass. The Goldstone bosons are then identified as the pions, kaons and the η particles, which have the same quantum numbers as the broken generators. These Goldstone bosons are interpreted as the mediators in the nuclear interactions.

6.1.1 The chiral effective Lagrangian

As mentioned above, we have to set up an effective Lagrangian containing all the symmetries of QCD. The chiral effective Lagrangian is given by an infinite series of terms. The terms contain an increasing number of derivatives. It is impossible to apply this Lagrangian to nucleon-nucleon scattering, when this generates an infinite number of Feynman diagrams. Weinberg showed that there is a systematic expansion of the nuclear amplitude in terms of $(Q/\Lambda_\chi)^\nu$, where Q denotes a momentum or pion mass, and $\Lambda\chi \approx 1GeV$ is the chiral symmetry breaking scale. For a given order ν the number of contributing terms is finite. This scheme is known as chiral perturbation theory.

In order to describe the effective NN interaction we write down all terms in the Lagrangian contributing to the given order we want, and consistent with the symmetries. The Feynman diagrams are generated by the terms in the Lagrangian.

The effective Lagrangian for NN interactions will finally be written as a sum of Lagrangians of pions, nucleons and pion-nucleon interactions

$$\mathcal{L} = \mathcal{L}_{\pi N} + \mathcal{L}_{\pi\pi} + \mathcal{L}_{NN}.$$

These terms are all given by a series of increasing chiral dimension,

$$\mathcal{L}_{\pi N} = \mathcal{L}_{\pi N}^{(1)} + \mathcal{L}_{\pi N}^{(2)} + \mathcal{L}_{\pi N}^{(3)} + \ldots,$$

$$\mathcal{L}_{\pi\pi} = \mathcal{L}_{\pi\pi}^{(2)} + \ldots,$$

$$\mathcal{L}_{NN} = \mathcal{L}_{NN}^{(0)} + \mathcal{L}_{NN}^{(2)} + \mathcal{L}_{NN}^{(4)} + \ldots.$$

The superscripts refer to the number of derivatives or pion mass insertions [23].

The chiral potential has the form

$$V_{\mathrm{2N}} = V_\pi + V_{\mathrm{cont}},$$

where V_{cont} denotes the short range term represented by NN contact interactions and V_π corresponds to the long range part associated with the pion exchange contribution. The pion exchange potential may be written as a sum of potentials of different amount of pion exchange

$$V_\pi = V_{1\pi} + V_{2\pi} + V_{3\pi} + \cdots.$$

The two pion exchange potential will not contribute until second leading order and the three pion exchange potential will not contribute until fourth order,

$$\begin{aligned} V_{1\pi} &= V_{1\pi}^{(0)} + V_{1\pi}^{(2)} + V_{1\pi}^{(3)} + V_{1\pi}^{(4)} + \ldots, \\ V_{2\pi} &= V_{2\pi}^{(2)} + V_{2\pi}^{(3)} + V_{2\pi}^{(4)} + \ldots, \\ V_{3\pi} &= V_{3\pi}^{(4)} + \cdots. \end{aligned}$$

We notice that n–pion exchange diagrams start to contribute at the order $(Q/\Lambda)^{2n-2}$.

The pion exchange potential at N^{3}LO is the sum

$$V_{1\pi}^{(0)} + V_{1\pi}^{(2)} + V_{1\pi}^{(3)} + V_{1\pi}^{(4)} + + V_{3\pi}^{(4)}. \tag{6.7}$$

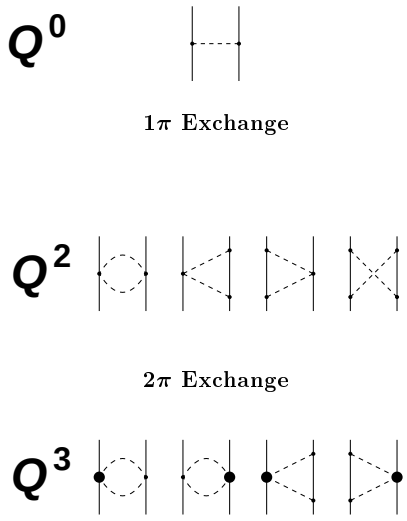

Figure 6.2: The most important irreducible one- and two-pion exchange contributions to the NN interaction up to order Q^3. Vertices denoted by small dots are from $\widehat{\mathcal{L}}^{(1)}_{\pi N}$, while large dots refer to $\widehat{\mathcal{L}}^{(2)}_{\pi N,\,\mathrm{ct}}$.

6.2 Derivation of nuclear interactions

Quantum chromodynamics (QCD) is the theory which for the moment is believed to explain the strong interactions among nucleons. The non-perturbative behavior of QCD in the low energy limit, makes it difficult to work with. Instead we work with effective field theories. In an effective field theory, we search for the relevant degrees of freedom, and integrate out the irrelevant degrees of freedom. In the nuclear limit we use nucleons and mesons as relevant degrees of freedom, while the quarks and gluons are frozen out. In the last section the chiral effective field theory was briefly explained. And a perturbation series of the nuclear potential was finally given. How do we derive such potentials? In this section we will try to derive some meson exchange potentials by using the phenomenological Lagrangians

$$\mathcal{L}_{ps} = g^{ps}\overline{\Psi}\gamma^5\Psi\phi^{(ps)},$$

$$\mathcal{L}_{s} = g^{s}\overline{\Psi}\Psi\phi^{(s)}, \tag{6.8}$$

and

$$\mathcal{L}_v = g^v \overline{\Psi}\gamma_\mu \Psi \phi_\mu^{(v)} + g^t \overline{\Psi}\sigma^{\mu\nu}\Psi\left(\partial_\mu \phi_\nu^{(v)} - \partial_\nu \phi_\mu^{(v)}\right), \tag{6.9}$$

for interactions with pseudoscalar mesons, scalar mesons and vector mesons respectively, see Ref. [10]. The coupling constants g^v, g^t, g^s and g^{ps} are purely phenomenological and constrained from nucleon-nucleon scattering data Ref. [24]. All the ϕ's correspond to the vector, scalar and pseudoscalar mesons, while Ψ corresponds to the spin 1/2 baryon fields.

The baryon fields are the solutions of the Dirac equation

$$i\gamma^\mu \partial_\mu \Psi - m\Psi = 0, \tag{6.10}$$

with the solution

$$\Psi(x) = \frac{1}{(2\pi)^{3/2}} \sum_{\mathbf{k}\sigma} u(k\sigma) e^{-ikx} a_{\mathbf{k}\sigma}, \tag{6.11}$$

where $u(k\sigma)$are the Dirac spinors

$$u(k\sigma) = \sqrt{\frac{E(k)+m}{2m}} \begin{pmatrix} \chi \\ \\ \frac{\boldsymbol{\sigma}\mathbf{k}}{E(k)+m}\chi \end{pmatrix},$$

with a being a fermion annihilation operator and χ the Pauli spinor. The term $E(k)$ is just the relativistic energy expression

$$E(k) = \sqrt{m^2 + |\mathbf{k}|^2}.$$

With the above Lagrangians and the Feynman diagram rules, see for example Refs. [21, 25], we can derive the two-body interaction with the interchange of a pion. The vertices are given by the pseudovector coupling

$$V^{pv} = \frac{f_\pi^2}{m_\pi^2} \frac{\overline{u}(p_1')\gamma_5\gamma_\mu(p_1 - p_1')^\mu u(p_1)\overline{u}(p_2')\gamma_5\gamma_\nu(p_2' - p_2)^\nu u(p_2)}{(p_1 - p_1')^2 - m_\pi^2}. \tag{6.12}$$

The numerator can be further evaluated by using the relationships

$$\gamma_\mu p^\mu u(p) = mu(p)$$
$$\overline{u}(p)\gamma_\mu p^\mu = m\overline{u}(p)$$

and $\{\gamma_5, \gamma_\mu\} = 0$, see Refs. [26, 27]. Let us calculate the terms involving p_1 and p_1' first, namely

$$\overline{u}(p_1')\gamma_5\gamma_\mu(p_1 - p_1')^\mu u(p_1) = m\overline{u}(p_1')\gamma_5 u(p_1) + \overline{u}(p_1')\gamma_\mu p_1'^\mu \gamma_5 u(p_1)$$
$$= 2m\overline{u}(p_1')\gamma_5 u(p_1).$$

The term term involving momenta p_2 and p_2' results in

$$\overline{u}(p_2')\gamma_5\gamma_\mu(p_2'-p_2)^\mu = -2m\overline{u}(p_2')\gamma_5 u(p_1).$$

We are now able to write down the coupling in momentum representation as

$$V^{pv} = -\frac{f_\pi^2}{m_\pi^2}4m^2\frac{\overline{u}(p_1')\gamma_5 u(p_1)\overline{u}(p_2')\gamma_5 u(p_2)}{(p_1-p_1')^2-m_\pi^2}. \tag{6.13}$$

Let us calculate the products $\overline{u}(p')\gamma_5 u(p)$. By inserting for the Dirac spinors and the γ_5 matrix, we see that

$$\begin{aligned}\overline{u}(p_1')\gamma_5 u(p_1) &= \sqrt{\frac{(E_1'+m)(E_1+m)}{4m^2}}\left(\begin{array}{cc}\chi^\dagger - \frac{\sigma_1\cdot\mathbf{p_1}}{E_1'+m}\chi^\dagger\end{array}\right)\left(\begin{array}{cc}0 & 1\\ 1 & 0\end{array}\right)\\ &\times\left(\begin{array}{c}\chi\\ \frac{\sigma_1\cdot\mathbf{p_1}}{E_1+m}\chi\end{array}\right)\\ &= \sqrt{\frac{(E_1'+m)(E_1+m)}{4m^2}}\left(\frac{\sigma_1\cdot\mathbf{p_1}}{E_1+m}-\frac{\sigma_1\cdot\mathbf{p_1'}}{E_1'+m}\right).\end{aligned}$$

Similarly,

$$\overline{u}(p_2')\gamma_5 u(p_1) = \sqrt{\frac{(E_2'+m)(E_2+m)}{4m^2}}\left(\frac{\sigma_2\cdot\mathbf{p}_2}{E_2+m}-\frac{\sigma_2\cdot\mathbf{p'}_2}{E_2'+m}\right).$$

It is convenient to operate in the center-of-mass system, where the total momentum is zero, $p_1=-p_2$ and $p_1'=-p_2'$ with $E_1=E_2$ and $E_1'=E_2'$. We can now write down the relativistic contribution in the center-of-mass frame to the nucleon-nucleon potential,

$$\begin{aligned}V^{pv} = &-\frac{f_\pi^2}{m_\pi^2}4m^2\frac{1}{(p_1-p_1')^2-m_\pi^2}\frac{(E_1+m)(E_1'+m)}{4m^2}\\ &\times\left(\frac{\sigma_1\cdot\mathbf{p}_1}{E_1+m}-\frac{\sigma_1\cdot\mathbf{p'}_1}{E_1'+m}\right)\left(\frac{\sigma_2\cdot\mathbf{p}_1}{E_1+m}-\frac{\sigma_2\cdot\mathbf{p'}_1}{E_1'+m}\right).\end{aligned} \tag{6.14}$$

This work is done in the non relativistic limit, where $E=\sqrt{m^2+p^2}\approx m$ to lowest order. The energies E_1 and E_1' are approximately the same. We have now also an approximation to the non relativistic nucleon-nucleon interaction

$$\begin{aligned}V^{pv} &= -\frac{f_\pi^2}{m_\pi^2}4m^2\frac{1}{\mathbf{k}^2+m^2}\frac{2m\cdot 2m}{4m^2}\frac{\sigma_1}{2m}\cdot(\mathbf{p}_1-\mathbf{p'}_1)\frac{\sigma_2}{2m}\cdot(\mathbf{p}_1-\mathbf{p'}_1)\\ &= -\frac{f_\pi^2}{m_\pi^2}\frac{(\sigma_1\cdot\mathbf{k})(\sigma_2\cdot\mathbf{k})}{\mathbf{k}^2+m_\pi^2}\tau_1\cdot\tau_2,\end{aligned} \tag{6.15}$$

where $\mathbf{k}$ is the transfered momentum, $(p_1 - p_1')^2 = -\mathbf{k}^2$. The τs are Pauli isospin matrices. The exchange terms is omitted.

If we want Eq. (6.15) expressed in coordinate representation we do a Fourier transform of the equation

$$V^{pv}(r) = \int \frac{d^3k}{(2\pi)^3} e^{i\mathbf{kr}} V^{pv}(k),$$

which results in

$$V^{pv}(r) = \frac{f_\pi^2}{m_\pi^2} \boldsymbol{\tau}_1 \cdot \boldsymbol{\tau}_2 \sigma_1 \cdot \nabla \sigma_2 \cdot \nabla \int \frac{d^3k}{(2\pi)^3} e^{i\mathbf{kr}} \frac{1}{\mathbf{k}^2 + m_\pi^2}.$$

In coordinate representation $\mathbf{k}$ becomes the differentiation operator ∇. The integral over k has to be solved by Cauchy's residue theorem, resulting in

$$\begin{aligned}
&\int \frac{d^3k}{(2\pi)^3} e^{i\mathbf{kr}} \frac{1}{k^2 + m_\pi^2} = \int d\Omega \int \frac{dk}{(2\pi)^3} e^{ikr\cos(\theta)} k^2 \frac{1}{k^2 + m_\pi^2} \\
&= \int_0^\pi d\theta \int \frac{dk}{(2\pi)^2} e^{ikr\cos(\theta)} k^2 \frac{1}{k^2 + m_\pi^2} \\
&= \int \frac{dk}{ikr(2\pi)^2} (e^{ikr} - e^{-ikr}) \frac{k^2}{k^2 + m_\pi^2} = \int \frac{dk}{ir(2\pi)^2} (e^{ikr} - e^{-ikr}) \frac{k}{(k + im_\pi)(k - im_\pi)} \\
&= \frac{e^{-m_\pi r}}{2\pi r}.
\end{aligned}$$

We obtain then

$$V^{pv}(r) = \frac{f_\pi^2}{2\pi m_\pi^2} \boldsymbol{\tau}_1 \cdot \boldsymbol{\tau}_2 \sigma_1 \cdot \nabla \sigma_2 \cdot \nabla \frac{e^{-m_\pi r}}{r}.$$

Doing the differentiation gives us

$$\frac{f_\pi^2}{3\pi} \left(\sigma_1 \cdot \sigma_2 + \big(1 + \frac{3}{m_\pi r} + \frac{3}{(m_\pi r)^2}\big) S_{12} \right).$$

Where $S_{12} = (3\hat{r}\hat{r} - \delta_{ij})\sigma_1\sigma_2$, where $\hat{r} = \mathbf{r}/|r|$. To get the full pion-exchange nucleon-nucleon potential, we have to add the exchange term and the isospin dependence.

By doing similar derivations for the scalar and vector meson exchange Eqs. (6.8) and (6.9), we get the potential for exchange of ω bosons on the form

$$V^\omega = g_{\omega NN}^2 \frac{1}{\mathbf{k}^2 + m_\omega^2} \left(1 - 3\frac{\mathbf{LS}}{2M_N^2} \right). \tag{6.16}$$

For the ρ meson the potential becomes

$$V^\rho = g_{\rho NN}^2 \frac{\mathbf{k}^2}{\mathbf{k}^2 + m_\rho^2} \left(-2\sigma_1\sigma_2 + S_{12}(\hat{k}) \right) \tau_1\tau_2. \tag{6.17}$$

6.3 V_{low-k}

Since there is a repulsive part in all of the different nucleon-nucleon potentials, even in N^{3}LO, which is derived from the chiral symmetries of QCD, it is necessary to renormalize it. One of the renormalization procedures is called V_{low-k}. This method separates the Hilbert space in a low momentum part and a high momentum part, see Ref. [28]. This is done by introducing a cutoff in momentum space where all states with momenta higher than the cutoff belong to the high momentum space.

As explained above, the nucleon-nucleon interaction becomes highly repulsive at small interparticle distances. By renormalizing the potential the repulsive and the non perturbative part of it "get swept under the carpet" as Zee in Ref. [29] says it. There are many ways to renormalize the potential, or to get "rid off" the high momentum part, all of them must have one thing in common. The renormalized potential should give an accurate description of the low energy nucleon-nucleon scattering data.

The renormalization procedure is based on two steps, see Ref. [30] for details. The first step is to diagonalize the momentum space for relative momenta. We transform k from $k \in [0, \infty)$ to $k \in [0, \lambda]$, with a typical value of λ approximately 2 fm^{-1}. The renormalized potential, V_{low-k}, is dependent on the cutoff.

For deriving the effective potential we first have to consider the full many-body system described by Schrödinger's equation

$$H|\Psi\rangle = E|\Psi\rangle. \tag{6.18}$$

The Hamiltonian is separated in an unperturbed part and a perturbed part as in chapter 4. The separation is written again as

$$H = H_0 + H_I, \tag{6.19}$$

where H_I denotes the perturbed Hamiltonian and describes the interaction part. The first part of constructing an effective Hamiltonian is to use the same projection operators as in chapter 4, P and Q, that project onto the low energy state and the high energy state, respectively. The projection operators still satisfy the properties of Eq. (4.5)

$$\begin{aligned} &P^2 = P, \\ &Q^2 = Q, \\ &P + Q = 1, \\ &PQ = QP = 0, \\ &[H_0, P] = [H_0, Q] = 0, \end{aligned}$$

and

$$QH_0P = PH_0Q = 0.$$

By using the projection operators the Hamiltonian may be written as

$$H = (P+Q)H(P+Q) = PHP + PHQ + QHP + QHQ. \tag{6.20}$$

The Schrödinger equation can then be written in matrix form as

$$\begin{pmatrix} PHP & PHQ \\ QHP & QHQ \end{pmatrix} \begin{pmatrix} P|\Psi\rangle \\ Q|\Psi\rangle \end{pmatrix} = E \begin{pmatrix} P|\Psi\rangle \\ Q|\Psi\rangle \end{pmatrix}. \tag{6.21}$$

There exists two main methods for solving the effective Hamiltonian. The first is the Bloch-Horowitz [31, 32] scheme where the effective Hamiltonian turns out to be dependent on the exact energy eigenvalue one is solving for. The second method is the so-called Lee-Suzuki method Refs. [33, 34]. The two methods are thoroughly compared in Ref. [35]. Both of the methods result in an effective Hamiltonian on the form

$$H_{eff} = PHP \tag{6.22}$$

The solution of the Bloch-Horowitz effective Hamiltonian is

$$\mathcal{H}_{eff}^{BH} = P(H + H\frac{1}{E - QHQ}H)P, \tag{6.23}$$

and the corresponding eigenvalue problem

$$P(H + H\frac{1}{E - QHQ}H)PP|\Psi\rangle = EP|\Psi\rangle \tag{6.24}$$

has to be solved by a self consistent treatment.

The Lee-Suzuki method avoids the difficulties with the energy eigenvalue in the effective Hamiltonian by doing a similarity transformation of the Hamiltonian in Eq. (6.21) to an upper diagonal block matrix as

$$H^{LS} = \begin{pmatrix} P\mathcal{H}P & P\mathcal{H}Q \\ 0 & Q\mathcal{H}Q \end{pmatrix} = X^{-1}HX. \tag{6.25}$$

The condition for $P\mathcal{H}P$ to be the P space effective Hamiltonian is that

$$QX^{-1}HXP = 0. \tag{6.26}$$

The choice of X is crucial since different choices of X lead to different effective interactions, Lee and Suzuki in Ref. [33] made the ansatz of

$$\begin{aligned} X &= e^{\omega} \\ \mathcal{H} &= e^{-\omega}He^{\omega}, \end{aligned} \tag{6.27}$$

where ω is the so-called wave operator. It connects the P and Q spaces in the sense that it transform the state $P|\Psi\rangle$ to the state $Q|\Psi\rangle$. With the wave operator on the form $\omega = Q\omega P$ the condition (6.26) is satisfied. This will also constrain the matrix X by the following properties of the wave operator

$$\begin{aligned} P\omega P &= PQ\omega PP = 0, \\ Q\omega Q &= QQ\omega PQ = 0, \\ P\omega Q &= PQ\omega QQ = 0, \end{aligned} \tag{6.28}$$

and

$$\omega^2 = Q\omega PQ\omega P = 0.$$

The expansion of X will then consist of just two terms

$$X = e^{\omega} = 1 + \omega = 1 + Q\omega P. \tag{6.29}$$

The four parts of of the Hamiltonian matrix in Eq. (6.21) will then be expressed as

$$\begin{aligned} P\mathcal{H}P &= PHP + PH_IQ\omega P, \\ P\mathcal{H}Q &= PH_IQ, \\ Q\mathcal{H}Q &= QHQ - \omega PH_IQ, \end{aligned} \tag{6.30}$$

and

$$Q\mathcal{H}P = QH_IP + QHQ\omega - \omega PHP - \omega PH_IQ\omega.$$

With Eqs. (6.3) and (6.30) we get an equation for the wave operator such as

$$QH_IP + QHQ\omega - \omega PHP - \omega PH_IQ\omega = 0. \tag{6.31}$$

If we have a solution for ω, we can insert it in Eq. (6.27) and obtain the effective Hamiltonian

$$H_{eff} = PHP + PH_IQ\omega P. \tag{6.32}$$

By defining the P space effective interaction operator

$$V_{eff} = H_{eff} - PH_0P = PH_IP + PH_IQ\omega, \tag{6.33}$$

the P space eigenvalue problem can be written as

$$H_{eff}|\psi_\mu\rangle = (PH_0P + V_{eff})|\psi_\mu\rangle = E_\mu|\psi_\mu\rangle. \tag{6.34}$$

The wave operator can be solved in terms of the eigenvalue and eigenstates E_μ and $|\psi_\mu\rangle$ as

$$\omega(E_\mu) = \sum_{\mu=1}^{d} \frac{1}{E_\mu - QHQ} QH_IP|\psi_\mu\rangle\langle\tilde{\psi}_\mu|, \tag{6.35}$$

where $\langle\tilde{\psi}_\mu|$ is the bi orthogonal state corresponding to $|\psi_\mu\rangle$. There are various methods for solving the non-linear equation for the wave operator. For the two body-problem, we can obtain a desired number of eigenvalues to a given numerical precision. These eigenstates can be used to compute ω.

Chapter 7

Coupled Cluster Theory

Coupled cluster theory was developed by Fritz Coester and Hermann Kümmel, [36] and [37]. It is a method used to describe many-body systems. The method starts with a ground state Slater determinant, as the Slater determinant below, Eq.(7.1), which corresponds to a system consisting of four particles

$$\Phi_0 = \frac{1}{\sqrt{4!}} \begin{vmatrix} \phi_i(x_1) & \phi_j(x_1) & \phi_k(x_1) & \phi_l(x_1) \\ \phi_i(x_2) & \phi_j(x_2) & \phi_k(x_2) & \phi_l(x_2) \\ \phi_i(x_3) & \phi_j(x_3) & \phi_k(x_3) & \phi_l(x_3) \\ \phi_i(x_4) & \phi_j(x_4) & \phi_k(x_4) & \phi_l(x_4) \end{vmatrix}. \tag{7.1}$$

A convenient shorthand notation for the Slater determinant consists of a Dirac-notation ket containing only the diagonal elements of the Slater determinant, see Ref. [4]. The ket vector corresponding to Eq. (7.1) would be written as

$$|\phi_i(x_1)\phi_j(x_2)\phi_k(x_3)\phi_l(x_4)\rangle. \tag{7.2}$$

This independent particle model does not consider the effects from the interactions beyond the uncorrelated wavefunction Φ_0 we get by filling the N single-particle orbitals with lowest energy. To include the effects beyond the uncorrelated wavefunction we make an ansatz and write the coupled cluster wavefunction as

$$\Psi = e^T \Phi_0, \tag{7.3}$$

where T is a cluster operator, not to be confused with the kinetic energy and $|\Phi_0\rangle$ is our reference vacuum. The cluster operator T is a linear combination of different types of excitations and written as

$$T = T_1 + T_2 + T_3 + \cdots \tag{7.4}$$

The symbol T_1 is an operator of all single excitations, and T_2 the operator of all double excitations, and so on. By the formalism of the second quantization the excitation

operators are expressed as

$$T_1 = \sum_{ia} t_i^a a_a^\dagger a_i \tag{7.5}$$

and

$$T_2 = \frac{1}{4} \sum_{ijab} t_{ij}^{ab} a_a^\dagger a_b^\dagger a_j a_i. \tag{7.6}$$

More generally an $n-$orbital cluster operator may be defined as

$$T_n = \left(\frac{1}{n!}\right)^2 \sum_{ij\ldots ab\ldots} t_{ij\ldots}^{ab\ldots} a_a^\dagger a_b^\dagger \ldots a_j a_i. \tag{7.7}$$

The new correlated wavefunction is a linear expansion of several Slater determinants which are considered as excitations of $|\Phi_0\rangle$. The cluster amplitudes, t_i^a, t_{ij}^{ab} etc., are to be determined via the Schrödinger equation, see for instance Ref. [4].
The new wavefunction $|\Psi\rangle$ satisfies the Schrödinger equation as written below

$$H|\Psi\rangle = He^T|\Phi_0\rangle = Ee^T|\Phi_0\rangle = E|\Psi\rangle.$$

To obtain an expression for the energy, the reference wave-function Φ_0 is multiplied from left with the Schrödinger. We obtain

$$\langle\Phi_0|He^T|\Phi_0\rangle.$$

However it has turned out to be convenient to multiply the Schrödinger equation, Eq. (7) with e^{-T} and then do a left-projection by the reference Φ_0, to get

$$E = \langle\Phi_0|e^{-T}He^T|\Phi_0\rangle. \tag{7.8}$$

By using the Campbell-Baker-Hausdorff formula on $e^{-T}He^T$, Eq. (7.8) transforms to

$$E = \langle\Phi_0|H+[H,T_1]+[H,T_2]+\frac{1}{2}[[H,T_1],T_1]+\frac{1}{2}[[H,T_2],T_2]+[[H,T_1],T_2]+\cdots|\Phi_0\rangle.$$

We have here truncated the cluster operator at T_2. The above expression is valid even at higher truncations as long as the Hamiltonian just consists of a two body operator. Different truncations are denoted by short-hand notations, for instance a truncation on T_1 is called a CCS approach, a truncation on T_2 a CCSD approach and a truncation on T_2 without considering the T_1 amplitudes is called a CCD approach.

In order to find the energy of the system we need to determine the amplitudes t_i^a and t_{ij}^{ab}. This is done by using the orthogonality properties

$$\langle \Phi_i^a | e^{-T} H e^T | \Phi_0 \rangle = 0, \tag{7.9}$$

and

$$\langle \Phi_{ij}^{ab} | e^{-T} H e^T | \Phi_0 \rangle = 0. \tag{7.10}$$

The above equations are to be derived in the following sections. Since we in this work have truncated the cluster operator at T_2, the equations (7.9) and (7.10) are the only equations needed in order to determine the cluster amplitudes t_i^a and t_{ij}^{ab}.

7.1 The CCSD energy equation

The energy problem simplifies when the normalized Hamiltonian, H_N, according to the quasiparticle formalism, is used, see Eq. (3.17). In the last section an expansion on $e^{-T}He^T$ was derived by the Campbell-Baker-Hausdorff formula. When our Hamiltonian is at most a two particle operator, this expression will be truncated at

$$\begin{aligned} e^{-T} H_N e^T &= H_N + [H_N, T_1] + [H_N, T_2] + \\ &\frac{1}{2}[[H_N, T_1], T_1] + \frac{1}{2}[[H_N, T_2], T_2] + [[H_N, T_1], T_2], \end{aligned} \tag{7.11}$$

where

$$H_N = \sum_{\alpha\beta} f_{\alpha\beta} N(a_\alpha^\dagger a_\beta) + \frac{1}{4} \sum_{\alpha\beta\gamma\delta} v_{\alpha\beta\gamma\delta} N(a_\alpha^\dagger a_\beta^\dagger a_\delta a_\gamma) \tag{7.12}$$

is the normal ordered Hamiltonian as in chapter 3, with

$$f_{\alpha\beta} = \langle \alpha | h | \beta \rangle + \frac{1}{4} \sum_i \langle \alpha i | v | i \beta \rangle \text{ and } v_{\alpha\beta\gamma\delta} = \langle \alpha\beta | v | \gamma\delta \rangle.$$

The first order correction to the energy,

$$E_0 = \sum_i \langle i | h | i \rangle + \frac{1}{2} \sum_{ij} \langle ij | v | ij \rangle,$$

see Eq.(3.17), is left out. By taking the expectation value of the expanded normal ordered Hamiltonian, Eq. (7.11), with the reference vacuum, Φ_0, we see that the first term, H_N of the expansion in Eq. (7.11) falls out. However the H_N term will contribute in the amplitude equations.

We will now go thoroughly through the terms in Eq. (7.11) and their expectation values with Φ_0. We start with the commutator of H_1 and T_1

$$[H_N, T_1] = H_N T_1 - T_1 H_N \tag{7.13}$$

Let us first calculate $\langle \Phi_0 | H_N T_1 | \Phi_0 \rangle$,

$$\sum_{\alpha\beta\gamma\delta} \sum_{\substack{i\in holes,\\ a\in particles}} \Big[f_{\alpha\beta} t_i^a \langle \Phi_0 | \, N\big(\overbrace{a_\alpha^\dagger \overbrace{a_\beta}\big) a_a^\dagger} a_i \, | \Phi_0 \rangle + \tag{7.14}$$

$$v_{\alpha\beta\gamma\delta} t_i^a \sum_{all\ contractions} \langle \Phi_0 | N\big(a_\alpha^\dagger a_\beta^\dagger a_\delta a_\gamma\big) a_a^\dagger a_i | \Phi_0 \rangle \Big] = \sum_{\substack{a\in particles,\\ i\in holes}} f_{ia} t_i^a.$$

The second term before the equal sign in Eq. (7.14) becomes zero, because no fully contracted terms can be generated from it. We will always be left with one creation operator and one annihilation operator in the two-body term in Eq. (7.14) which are already normal ordered and hence annihilates the reference vacuum. The term $\langle \Phi_0 | T_1 H_N | \Phi_0 \rangle$ is zero, the normal ordered Hamiltonian, H_N annihilates the vacuum reference state, Φ_0. From this we conclude that all terms with a cluster operator to the left of the normal ordered Hamiltonian become zero when taking the expectation value with Φ_0. By using these relations, we write the energy equation as

$$E = \langle \Phi_0 | H_N T_1 + H_N T_2 + \frac{1}{2} H_N T_1^2 | \Phi_0 \rangle. \tag{7.15}$$

The other terms beside $H_N T_1$ that contribute to the energy are

$$H_N T_2 \tag{7.16}$$

and

$$\frac{1}{2} H_N T_1^2. \tag{7.17}$$

For the terms in Eqs. (7.16) and (7.17) it is only the two particle operator of the Hamiltonian that contributes.

Let us first consider $H_N T_2$:

$$\langle\Phi_0|H_N T_2|\Phi_0\rangle = \frac{1}{16}\sum_{\alpha\beta\gamma\delta}\sum_{\substack{ab\in particles\\ij\in holes}}\Big(v_{\alpha\beta\gamma\delta}t_{ij}^{ab}\langle\Phi_0|\,N\big(\overbrace{a_\alpha^\dagger a_\beta^\dagger a_\delta a_\gamma}\big)\overbrace{a_a^\dagger a_b^\dagger a_j a_i}\,|\Phi_0\rangle$$

$$+ v_{\alpha\beta\gamma\delta}t_{ij}^{ab}\langle\Phi_0|\,N\big(\overbrace{a_\alpha^\dagger a_\beta^\dagger a_\delta a_\gamma}\big)\overbrace{a_a^\dagger a_b^\dagger a_j a_i}\,|\Phi_0\rangle + v_{\alpha\beta\gamma\delta}t_{ij}^{ab}\langle\Phi_0|\,N\big(\overbrace{a_\alpha^\dagger a_\beta^\dagger a_\delta a_\gamma}\big)\overbrace{a_a^\dagger a_b^\dagger a_j a_i}\,|\Phi_0\rangle$$

$$+ v_{\alpha\beta\gamma\delta}t_{ij}^{ab}\langle\Phi_0|\,N\big(\overbrace{a_\alpha^\dagger a_\beta^\dagger a_\delta a_\gamma}\big)\overbrace{a_a^\dagger a_b^\dagger a_j a_i}\,|\Phi_0\rangle\Big) = \frac{1}{4}\sum_{\substack{ab\in particles\\ij\in holes}} v_{ijab}t_{ij}^{ab}. \tag{7.18}$$

The last expectation value, Eq. (7.17), is calculated by the same method to be

$$\frac{1}{2}\langle\Phi_0|H_N T_1^2|\Phi_0\rangle = \frac{1}{2}\sum_{\substack{a,b\in particles,\\ i,j\in holes}} v_{ijab}t_i^a t_j^b. \tag{7.19}$$

We sum the terms contributing to the energy, in the coupled cluster single and doubly excited approximation, CCSD;

$$E_{CCSD} = \sum_{i,a} f_{ia}t_i^a + \frac{1}{4}\sum_{\substack{i,j\\a,b}} v_{ijab}t_{ij}^{ab} + \frac{1}{2}\sum_{\substack{i,j,\\a,b}} v_{ijab}t_i^a t_j^b, \tag{7.20}$$

where i, j act only in the hole space and a, b act in the particle space. The convention where, a, b, c, d indicate single-particle state and i, j, k and l indicate single-hole states will be used hereafter.
As mentioned above, this energy relation is valid even if the cluster operator is not truncated at T_2, when the Hamiltonian is a two-body operator. The cluster operators such as T_3 will then contribute indirectly through the amplitude equations.

A problem with the coupled cluster Hamiltonian $\bar{H} = e^{-T}He^{T}$, is that it is not Hermitian.

$$\left(e^{-T}He^{t}\right)^\dagger = \left(e^{T}\right)^\dagger H\left(e^{-T}\right)^\dagger = e^{T^\dagger}H^{-T^\dagger} \neq e^{-T}He^{T}.$$

When T is not truncated the eigenvalue spectrum of the coupled cluster Hamiltonian is identical to the original Hamiltonian. Even when the operator T is truncated the coupled cluster energy tends to approximate the exact expectation value. When solving the eigenvalue problem with the coupled cluster Hamiltonian we will have a

non-symmetric Hamiltonian as the CCSD Hamiltonian on the form

$$\begin{pmatrix} E_{CCSD} & \bar{H}_{0S} & \bar{H}_{0D} \\ 0 & \bar{H}_{SS} & \bar{H}_{SD} \\ 0 & \bar{H}_{DS} & \bar{H}_{DD} \end{pmatrix},$$

where E_{CCSD} is the groundstate energy as in Eq. (7.20). The left-hand eigenvalue problem will be different from the right-hand eigenvalue problem, where the left-hand eigenvector $\langle\mathcal{L}|$ is defined as

$$\langle\mathcal{L}| = \langle\Phi_0|\mathcal{L}.$$

The operator $\mathcal{L}$ may be defined in analogy to the cluster operator, as a sum of excitation operators

$$\mathcal{L} = 1 + \mathcal{L}_1 + \mathcal{L}_2 + \cdots .$$

The leading term of 1 is required to let the left and right handed eigenvectors have unit overlap with one another. The $\mathcal{L}_n$ terms are defined as

$$\mathcal{L}_n = \left(\frac{1}{n!}\right)^2 \sum_{ij\ldots ab\ldots}^{n} l_{ab\ldots}^{ij\ldots} a_i^\dagger a_j^\dagger \ldots a_b a_a$$

To determine the left hand groundstate eigenvector reduces to determine the amplitudes $l_{ab\ldots}^{ij\ldots}$. We may then write the groundstate coupled cluster energy as

$$\langle\Phi_0|\mathcal{L}\bar{H}|\Phi_0\rangle,$$

where left and right wavefunctions are assumed to be normalized according to $\langle\Phi_0|\mathcal{L}|\Phi_o\rangle = 1$. The eigenvalue problem may also be extended to include excited states, we generalize the right handed eigenvalue problem to the form

$$\bar{H}\mathcal{R}(m)|\Phi_0\rangle = E_m\mathcal{R}(m)|\Phi_0\rangle,$$

where the term $\mathcal{R}(m) = \mathcal{R}_0(m) + \mathcal{R}_1(m) + \cdots$, represents a cluster operator for the m'th excited state. For the groundstate, the operator $\mathcal{R}(0)$ should equal the unit operator, 1. The left handed problem is written in a similar form,

$$\langle\Phi_0|\mathcal{L}(m)\bar{H} = E\langle\Phi_0|\mathcal{L}(m).$$

The left and right-handed excited states should satisfy the orthonormality condition $\langle\Phi_0|\mathcal{L}(m)\mathcal{R}(n)|\Phi_0\rangle = \delta_{mn}$, such that the excited energy can be computed from

$$E_m = \langle\Phi_0|\mathcal{L}(m)\bar{H}\mathcal{R}(m)|\Phi_0\rangle.$$

7.2 The CCSD amplitude equations

In the last section we saw that in order to find the energy, we have to decide the amplitudes t_i^a and t_{ij}^{ab} by the equations (7.9) and (7.10) . Remember the equation for solving the t_i^a amplitude,

$$\langle \Phi_i^a | e^{-T} H e^T | \Phi_0 \rangle$$

and the equation for solving the t_{ij}^{ab} amplitude,

$$\langle \Phi_{ij}^{ab} | e^{-T} H e^T | \Phi_0 \rangle.$$

Computing Eqs. (7.9) and (7.10) is much more tedious, and will require much more terms than the equation for the energy, see Eq. (7.20), since they are not an expectation value of the reference vacuum, but combine an excited state and the reference vacuum, Φ_0. There are more creation and destruction operators to handle because of the excited states which are defined as

$$\langle \Phi_i^a | = \langle \Phi_0 | a_i^\dagger a_a$$

for a singly excited state and as

$$\langle \Phi_{ij}^{ab} | = \langle \Phi_0 | a_j^\dagger a_i^\dagger a_a a_b$$

for a doubly excited state. In the so-called j-scheme representation [38, 39] we have to remember that an annihilation operator is written on the form

$$\tilde{a}_{jm} = (-1)^{j-m} (a_{jm}^\dagger)^\dagger,$$

where j is the angular momentum and m its projection. The leading term in the equation for the amplitudes is just H_N as seen from Eqs. (7.11), (7.9) and (7.10). Only the one-particle part of the Hamiltonian contributes to the first leading term of the singly excited amplitude, $\langle \Phi_i^a | e^{-T} H e^T | \Phi_0 \rangle$, as seen below

$$\langle \Phi_i^a | = \langle \Phi_0 | a_i^\dagger a_a e^{-T} H e^T | \Phi_0 \rangle = f_{ai}. \tag{7.21}$$

While the first leading term in $\langle \Phi_{ij}^{ab} | e^{-T} H e^T | \Phi_0 \rangle$ is

$$\langle \Phi_0 | a_i^\dagger a_j^\dagger a_b a_a e^{-T} H e^T | \Phi_0 \rangle = v_{abij}. \tag{7.22}$$

The process is more tedious when we calculate parts including the cluster operators, by Wick's theorem we find the T_1 amplitude equation to be

$$0 = f_{ai} + \sum_c f_{ac} t_i^c - \sum_k f_{ki} t_k^a + \sum_{kc} \langle ka|v|ci\rangle t_k^c + \sum_{kc} f_{kc} t_{ik}^{ac} + \frac{1}{2} \sum \langle ka|v|cd\rangle t_{ki}^{cd} -$$
$$\frac{1}{2} \sum_{klc} \langle kl|v|ci\rangle t_{kl}^{ca} - \sum_{kc} f_{kc} t_i^c t_k^a - \sum_{klc} \langle kl|v|ci\rangle t_k^c t_l^a + \sum_{kcd} \langle ka|v|cd\rangle t_k^c t_i^d - \sum_{klcd} \langle kl|v|cd\rangle t_k^c t_i^d t_l^a +$$
$$\sum_{klcd} \langle kl|v|cd\rangle t_k^c t_{li}^{da} - \frac{1}{2} \sum_{klcd} \langle kl|v|cd\rangle t_{ki}^{cd} t_l^a - \frac{1}{2} \sum_{klcd} \langle kl|v|cd\rangle t_{kl}^{ca} t_i^d. \tag{7.23}$$

While the amplitude equation for T_2 results in

$$
\begin{aligned}
0 = &\langle ab|v|ij\rangle + \sum_c (f_{bc}t^{ac}_{ij} - f_{ac}t^{bc}_{ij}) - \sum_k (f_{kj}t^{ab}_{ik} - f_{ki}t^{ab}_{jk}) + \\
&\frac{1}{2}\sum_{kl}\langle kl|v|ij\rangle t^{ab}_{kl} + \frac{1}{2}\sum_{cd}\langle ab|v|cd\rangle t^{cd}_{ij} + P(ij)P(ab)\sum_{kc}\langle kb|v|cj\rangle t^{ac}_{ik} + \\
&P(ij)\sum_c \langle ab|v|cj\rangle t^c_i - P(ab)\sum_k \langle kb|v|ij\rangle t^a_k + \frac{1}{4}\sum_{klcd}\langle kl|v|cd\rangle t^{cd}_{ij}t^{ab}_{kl} + \\
&\frac{1}{2}P(ij)P(ab)\sum_{klcd}\langle kl|v|cd\rangle t^{ac}_{ik}t^{db}_{lj} - P(ab)\frac{1}{2}\sum_{kl}\langle kl|v|cd\rangle t^{ac}_{ij}t^{bd}_{kl} - \\
&P(ij)\frac{1}{2}\sum_{klcd}\langle kl|v|cd\rangle t^{ab}_{ik}t^{cd}_{jl} + P(ab)\frac{1}{2}\sum_{kl}\langle kl|v|ij\rangle t^a_k t^b_l + \\
&P(ij)\frac{1}{2}\sum_{cd}\langle ab|v|cd\rangle t^c_i t^d_j - P(ij)P(ab)\sum_{kc}\langle kb|v|ic\rangle t^a_k t^c_j + \\
&P(ab)\sum_{kc} f_{kc}t^a_k t^{bc}_{ij} + P(ij)\sum_{kc} f_{kc}t^c_i t^{ab}_{jk} - \\
&P(ij)\sum_{klc}\langle kl|v|ci\rangle t^c_k t^{ab}_{lj} + P(ab)\sum_{kcd}\langle ka|v|cd\rangle t^c_k t^{db}_{ij} + \\
&P(ij)P(ab)\sum_{kcd}\langle ak|v|dc\rangle t^d_i t^{bc}_{jk} + P(ij)P(ab)\sum_{klc}\langle kl|v|ic\rangle t^a_l t^{bc}_{jk} + \\
&P(ij)\frac{1}{2}\sum_{klc}\langle kl|v|cj\rangle t^c_i t^{ab}_{kl} - P(ab)\frac{1}{2}\sum_{kcd}\langle kb|v|cd\rangle t^a_k t^{cd}_{ij} - \\
&P(ij)P(ab)\frac{1}{2}\sum_{kcd}\langle kb|v|cd\rangle t^c_i t^a_k t^d_j + P(ij)P(ab)\frac{1}{2}\sum_{klc}\langle kl|v|cj\rangle t^c_i t^a_k t^b_l - \\
&P(ij)\sum_{klcd}\langle kl|v|cd\rangle t^c_k t^d_i t^{ab}_{lj} - P(ab)\sum_{klcd}\langle kl|v|cd\rangle t^c_k t^a_l t^{db}_{ij} + \\
&P(ij)\frac{1}{4}\sum_{klcd}\langle kl|v|cd\rangle t^c_i t^d_j t^{ab}_{kl} + P(ab)\frac{1}{4}\sum_{klcd}\langle kl|v|cd\rangle t^a_k t^b_l t^{cd}_{ij} + \\
&P(ij)P(ab)\sum_{klcd}\langle kl|v|cd\rangle t^c_i t^b_l t^{ad}_{kj} + P(ij)P(ab)\frac{1}{4}\sum_{klcd}\langle kl|v|cd\rangle t^c_i t^a_k t^d_j t^b_l .
\end{aligned}
\tag{7.24}
$$

The notation $P(ab)$ indicates a permutation operator whose action on a function, f, is defined as

$$P(pq)f(p,q) = f(p,q) - f(q,p). \tag{7.25}$$

For readers who want to see the entire calculation, we refer to Ref. [4].

7.3 Coupled cluster diagrams

As a relief there are easier ways to construct the coupled cluster energy and amplitude equations, that is with a diagrammatic approach. The equations can be represented by some sort of Feynman diagrams. The rules are not quite the same as in ordinary many-body physics. New rules are needed, and they are as follow

1. As in ordinary many-body perturbation, holes are represented by downward pointing lines and particles by upward pointing lines.

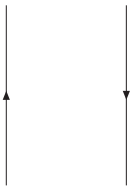

Figure 7.1: Diagrammatic representation of holes and particles, holes with an downward pointing arrow and particles with and upward pointing arrow.

2. The reference wavefunction $\Phi_0,$ is represented by empty space.

3. Dynamical operators such as the one particle and two particle part of the Hamiltonian are depicted by horizontal dashed lines as seen in Fig. 7.2.

Figure 7.2: Diagrammatic representation of the interaction line.

4. The cluster operators are depicted by solid horizontal lines as in Fig. 7.3

Figure 7.3: Depiction of the cluster operator.

5. The one particle component of the Hamiltonian is represented by a dashed interaction line capped by an $X,$ see Fig. 7.4.

6. Representation of the cluster operators is seen in Fig. 7.5. In the diagram representing the T_1 amplitude there is one incoming hole line and one outgoing particle line meeting at a solid horizontal line.

   The diagram representing T_2 consists of two incoming hole lines and two outgoing particle lines.

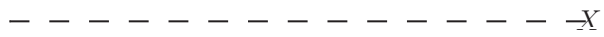

Figure 7.4: Depiction of the one particle component of the Hamiltonian.

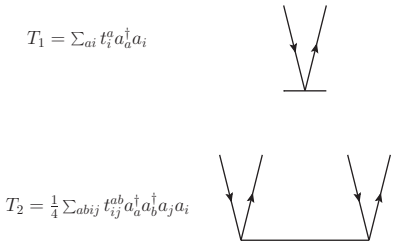

Figure 7.5: Diagrammatic representation of the cluster operators T_1 and T_2.

7. We label particle lines with $a, b, c, d, \cdots$. and all hole lines with $i, j, k, l, \cdots$ ..

8. We sum over internal lines, all indices associated with lines that begins and ends at operator interaction lines and do not extend to infinity above or below the diagram.

9. For each hole line, multiply with a factor of -1.

10. For each loop, multiply with a factor of -1. In Fig. 7.6 we have depicted the interpretations of loops in the coupled cluster diagrams. A loop is a route a long a series of directed lines that either returns to its beginning or begins at one external line and ends at another.

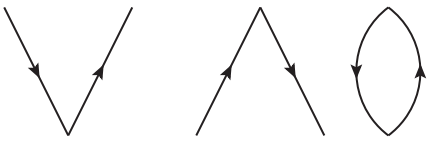

Figure 7.6: Three different types of loops in the coupled cluster diagrams.

11. For each pair of equivalent lines multiply with the factor $1/2$. An equivalent pair of lines are lines beginning at the same operator interaction line and ending at the same interaction line.

12. If there are n equivalent vertices's in the diagram, multiply with the factor $1/n!$.

13. For each pair of unique external hole or particle lines, multiply with the permutation operator $P(pq)$.

By using the above diagram rules it is possible to write diagrams corresponding to the energy equation and amplitude equations.
Like the diagrams for the energy equation in Eq. (7.15)

$$E = \langle \Phi_0 | H_N + H_N T_1 + H_N t_2 + \frac{1}{2} H_N T_1^2 + \ldots | \Phi_0 \rangle \tag{7.26}$$

can be evaluated with the above rules. The first term will not contribute since the operator is normalized and therefore will annihilate the vacuum state and give zero contribution.

We will now study how the second term

$$\langle \Phi_0 | H_N T_1 | \Phi_0 \rangle, \tag{7.27}$$

which may be depicted as a Feynman-Goldstone diagram.
Since we have the reference vacuum in both incoming and outgoing states there should be no external lines, meaning that there should not be any line neither below or above the two horizontal operator lines. The T_1 operator stands to the right, and its corresponding interaction line should be in the bottom of the diagram. Only the one particle operator contributes since with a two particle operator it is impossible to draw a diagram with just internal lines, see Fig. 7.7. In the second contribution,

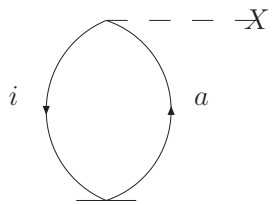

Figure 7.7: Diagrammatic representation of the first term in the ECCSD energy equation.

$$\langle \Phi_0 | H_N T_2 | \Phi_0 \rangle, \tag{7.28}$$

we have the reference vacuum in both incoming and outgoing state and therefore no external lines. Since the cluster operator is the rightmost one, the interaction line representing it should again be at the bottom. However, to this part only the two-particle operator of the Hamiltonian is contributing, something which should be reflected in the diagram. Figure 7.8 shows the diagram representing Eq. (7.28). The last part contributing to the $ECCSD$ energy equation is the term

$$\frac{1}{2} \langle \Phi_0 | H_N T_1^2 | \Phi_0 \rangle. \tag{7.29}$$

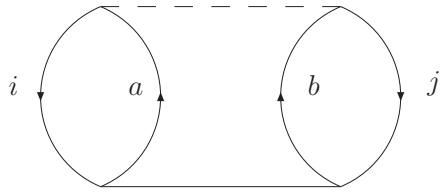

Figure 7.8: Diagrammatic representation of the second term in the ECCSD energy equation.

The interaction lines corresponding to the two cluster operators will again have to be drawn at the bottom of the diagram, the difference in this diagram, Fig. 7.9, from Fig. 7.8 is that the interaction line corresponding to the cluster operator is split since there are two one-excitation cluster operators to the right in Eq. (7.29). We can find

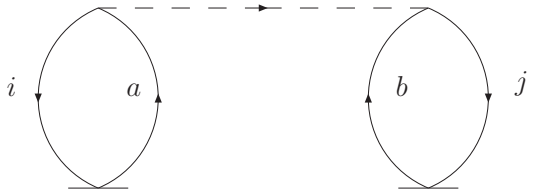

Figure 7.9: Diagrammatic representation of the last term in the ECCSD energy equation.

the T amplitude diagrams by using the commutators and the above diagram rules. However it is more practical to derive the amplitude equations from the amplitude diagrams. We start by drawing all topologically distinct diagrams with one external hole line and one external particle line for the T_1 amplitude equation. For the T_2 diagrams we must consider that there are two external hole lines and two external particle lines.

The first leading term in the equation corresponding to T_1 consists just of the Hamiltonian, and only the one particle part of it contributes. Its corresponding diagram is depicted in Fig. 7.10. All diagrams contributing to the T_1 equation can be seen in Fig. 7.11.
In Fig. 7.12 we depicted all diagrams contributing to the CCD equation, while the remaining parts in a CCSD approximation are depicted in Fig. 7.13.

To see the benefit with the diagrams, the $CCSD$ energy equation will now be computed from the diagrams. The total energy can be depicted as in Fig. 7.14
The way to interpret the diagrams is from the bottom to the upper part. The ingoing states are represented by a ket vector and the outgoing by the dual bra vector. In the

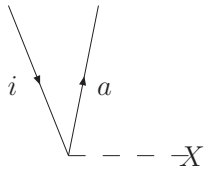

Figure 7.10: The diagram representing the first leading term in the T_1 amplitude equation.

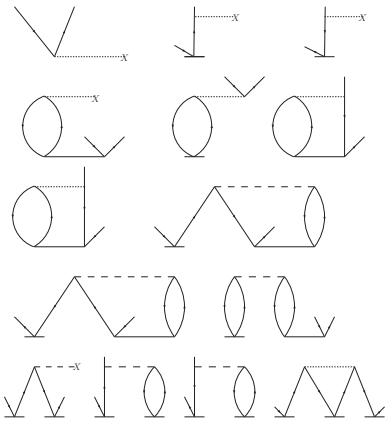

Figure 7.11: All diagrams contributing to the equation for solving the T_1 amplitude.

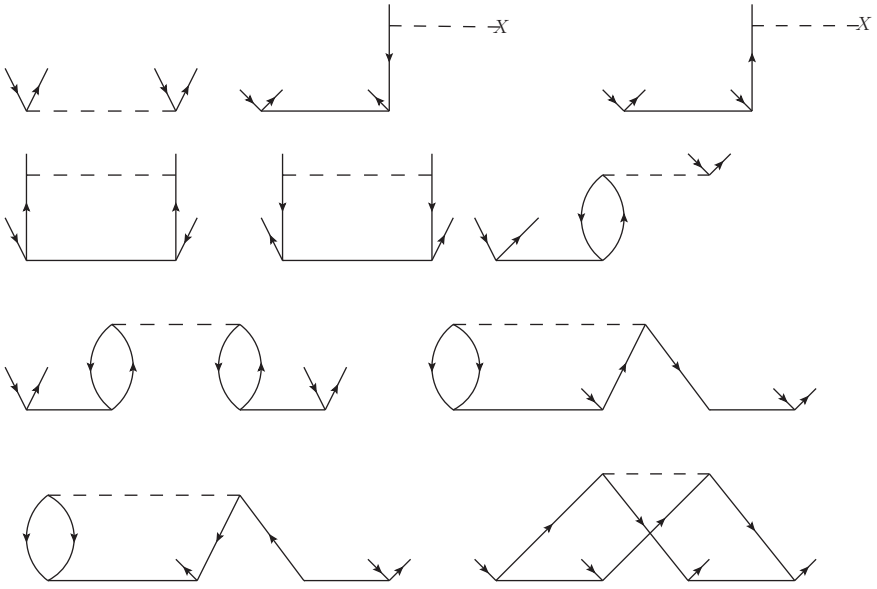

Figure 7.12: All diagrams contributing to the equation for solving the T_2 amplitude in the CCD approach.

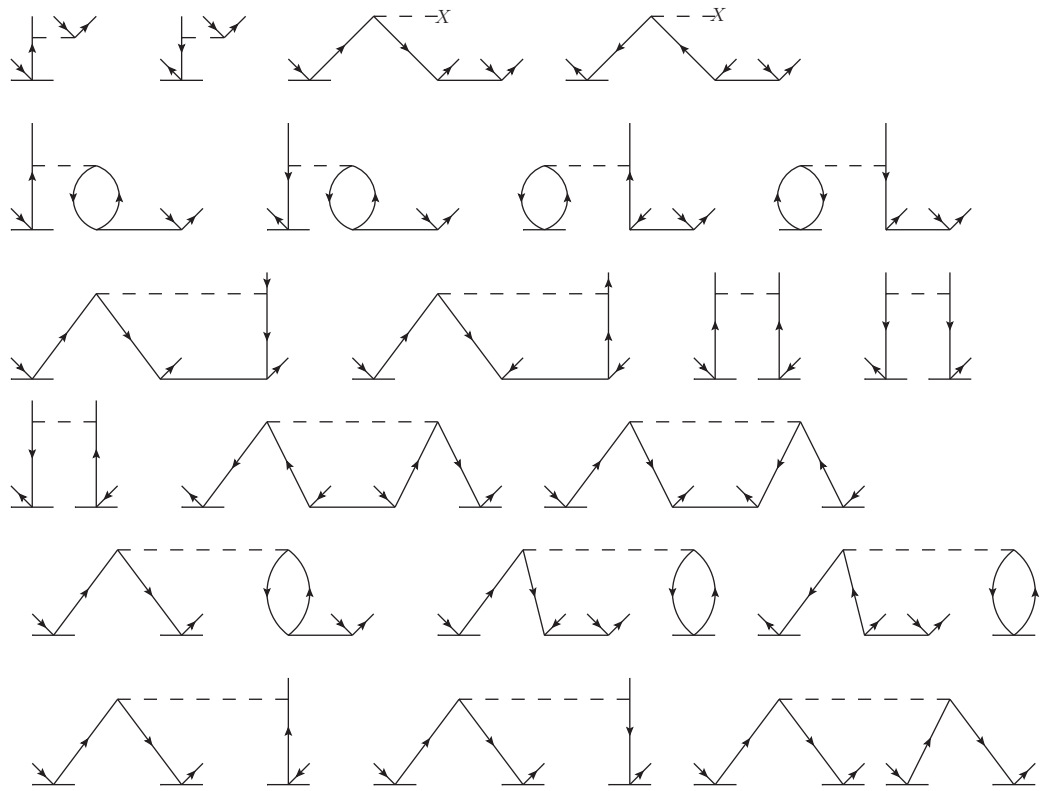

Figure 7.13: The diagrams remaining in a CCSD approach to the T_2 amplitude.

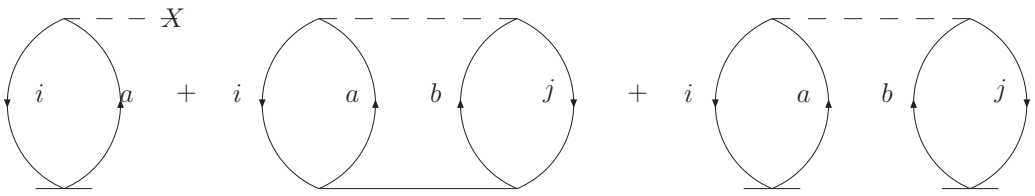

Figure 7.14: The diagrams representing the total $CCSD$ energy.

first diagram in Fig. 7.14 the one-excitation operator line is at the bottom. We label each internal particle and hole line and perform a sum over all hole and particle states. We have one hole line and one loop which together contributes as $(-1)^{1+1} = 1$. On top we have a one-body interaction line. We find that the first diagram in Fig. 7.14 should be understood as

$$\sum_{ai} f_{ia} t_i^a, \tag{7.30}$$

By using the above diagram rules to the second diagram in Fig. 7.14, we find its matrix elements to be

$$\frac{1}{4} \sum_{ijab} v_{ijab} t_{ij}^{ab}, \tag{7.31}$$

where $v_{ijab} = \langle ij|v|ab\rangle$. We have two loops and two hole lines which together contribute with the factor 1. We have two pairs of equivalent lines which together contribute with the factor $1/4$. A factor of $1/2$ for each pair of equivalent lines. With the same reasoning we write the last diagram in Fig. 7.14 as

$$\frac{1}{2} \sum_{ijab} \langle ij|v_N|ab\rangle t_i^a t_j^b = \frac{1}{2} \sum_{ijab} v_{ijab} t_i^a t_j^b. \tag{7.32}$$

The factor of $1/2$ appears because of two equivalent vertices. After summing up the energy, the total equation becomes

$$\sum_{ia} f_{ia} t_i^a + \frac{1}{4} \sum_{ijab} v_{ijab} t_{ij}^{ab} + \frac{1}{2} \sum_{ijab} v_{ijab} t_i^a t_j^b, \tag{7.33}$$

which is exactly the same as the equation got by using Wick's theorem.

7.4 Computation of the equations

This section will treat the computational approach for solving the amplitude equations as Eqs. (7.23) and (7.24). It is not always clear how one should approach the equations. A first approach could be to rearrange the equations to provide a more handy form. As an example the first few terms of Eq. (7.23), could be written as

$$0 = f_{ai} + f_{aa} t_i^a - f_{ii} t_i^a + \sum_c (1 - \delta_{ca}) f_{ac} t_i^c - \sum_k (1 - \delta_{ik}) f_{ik} t_k^a + \cdots \tag{7.34}$$

By defining

$$D_i^a = f_{ii} - f_{aa} \tag{7.35}$$

we rewrite Eq. (7.34) as

$$D_i^a t_i^a = f_{ai} + \sum_c (1-\delta_{ca}) f_{ac} t_i^c - \sum_k (1-\delta_{ik}) f_{ik} t_k^a + \cdots . \tag{7.36}$$

By also defining

$$D_{ij}^{ab} = f_{ii} + f_{jj} - f_{aa} - f_{bb} \tag{7.37}$$

the T_2 amplitude can be rewritten as

$$D_{ij}^{ab} t_{ij}^{ab} = \langle ab|v|ij\rangle + P(ab)\sum_c (1-\delta_{bc}) f_{bc} t_{ij}^{ac} - P(ij)\sum_k (1-\delta_{kj}) f_{kj} t_{ik}^{ab} + \cdots \tag{7.38}$$

The equations above have to be solved iteratively. A starting point for t_i^a and t_{ij}^{ab} may be obtained by setting all of the amplitudes on the right-hand side to zero. The initial guess for the amplitudes are then

$$t_i^a = f_{ai}/D_i^a, \tag{7.39}$$

for the T_1 amplitude and

$$t_{ij}^{ab} = \langle ab|v|ij\rangle / D_{ij}^{ab} \tag{7.40}$$

for the T_2 amplitude.
These initial guesses have to be inserted on the right-hand side of the equations and then subsequently used to obtain new amplitudes. This process is continued until an explicit convergence is reached.

In momentum space and a plane wave basis in addition to the sum over single-particle states in the energy and amplitude equations, we will also have to integrate over the momentum for each single-particle state. Holes have momentum less than the Fermi momentum k_f, while particles have momentum greater than k_f.

The single-particle functions φ are defined as plane-waves

$$\varphi = \frac{1}{\sqrt{\Omega}} e^{i\mathbf{kr}},$$

where the volume, Ω is infinite, k denotes the principal wave-number and r the radial coordinate. When we calculate interactions it is convenient to do a so-called partial wave-expansion. We expand the exponential as a sum of Legendre polynomials and spherical Bessel functions

$$e^{ikr} = \sum_{l=0}^{\infty} (2l+1) i^l j_l(kr) P_l(\Omega_{k,r}),$$

where the spherical Bessel functions $j_l(kr)$ depends on the radial part of the momentum and position vector, see appendix D.1 and D.2 for details about the functions. The Legendre polynomials P_l depends on $\Omega_{k,r} = \mathbf{k} \cdot \mathbf{r}/(|k||r|)$, which is the cosine angle between $\mathbf{k}$ and $\mathbf{r}$. The sum goes over orbital momentum l.

We saw in Eqs. (7.23) and (7.24) that there are many diagrams contributing to the amplitude equations, as many diagrams as terms in the equations. It requires a lot of time computing all these diagrams separately, therefore it is wise to factorize the diagrams. This can be done, since the coupled cluster diagrams do not have any denominators in their's expressions, in contrast to the diagrams in perturbation theory. Instead of computing the same factors several times, we compute it once and multiply it with the corresponding terms, as explained by Ref. [40]. In this work the factorization used is the same as the one used by Ref. [41].

7.5 Further analysis of the coupled cluster method

In the section on perturbation theory we derived the diagram rules and draw diagrams up to third order. In section 7.4 we showed how to solve the CCSD equations. With an initial guess for the T_2 amplitude as

$$\frac{\langle ab|v|ij\rangle}{f_{ij} - f_{ab}} \tag{7.41}$$

and insert it in the CCSD energy equation gives us

$$E_{T_2} = \frac{1}{4}\sum_{\substack{i,j\\a,b}} v_{ijab} t_{ij}^{ab} = \frac{1}{4}\sum_{\substack{i,j\\a,b}} \frac{\langle ij|v|ab\rangle\langle ab|v|ij\rangle}{f_{ij} - f_{ab}}, \tag{7.42}$$

which is exactly the same expression as the second order contribution to the energy in perturbation theory. By doing more of the iterations, the coupled cluster method will also include diagrams from third and fourth order in perturbation theory.

A convenient property of the coupled cluster method is that it is size consistent and size extensive. By size consistent we mean that computing the energy of two nuclei with an infinite distance between them is just to compute the two energies separately. As an example we consider two nuclei, A and B.

$$\begin{aligned} |\Phi_0\rangle &= |\Phi_0^A\rangle|\Phi_0^B\rangle \\ e^T|\Phi_0\rangle &= e^{T_A+T_B}|\Phi_0^A\rangle|\Phi_0^B\rangle = e^{T_A}|\Phi_0^A\rangle e^{T_B}|\Phi_0^B\rangle. \end{aligned} \tag{7.43}$$

With the Hamiltonian on the form $H = H_A + H_B$ the energy of the combined system sums up to

$$E_{CC} = E^A_{CC} + E^B_{CC}. \tag{7.44}$$

With size extensive means that the energy is linearly dependent on the number of particles present.

Chapter 8

The two-body matrix elements

Until now we have mostly been concerned with different theories applied in the project, in this part we will present how the calculations are done. In the first part we will show explicitly how matrix elements are calculated while we in the next sections we detail the calculations of the interactions.

8.1 Calculation of matrix elements

When computing matrix elements the Wigner-Eckart theorem has turned out to be very important. The theorem states that when calculating the matrix element of a spherical tensor it is allowed to do a separation in the part that only depends on the projection quantum numbers and a part that depends on the radial properties. The Wigner-Eckart theorem reads

$$\langle \alpha j m | T^{(k)}_{\kappa} | \beta j' m' \rangle = (-1)^{j-m} \begin{Bmatrix} j & k & j' \\ -m & \kappa & m' \end{Bmatrix} \langle \alpha j | T^{(k)} | \beta j' \rangle,$$

where the j's indicate angular momentum and the m's are the corresponding projections on a chosen z-axis, while k denotes the rank of the tensor T and κ is its projection. The curly bracket is a $6j$-symbol.
This theorem can be used to calculate two body matrix elements. Consider a product to two tensor operators, $T = T(1) \otimes T(2)$, acting on two independent subsystems denoted 1 and 2

$$\langle \alpha_1 j_1 \alpha_2 j_2 JM | T | \beta_1 j_1' \beta_2 j_2' JM \rangle. \tag{8.1}$$

By uncoupling the wave functions applying Wigner Eckart theorem we can rewrite the matrix element in Eq. (8.1) as

$$\begin{aligned}
&\langle \alpha_1 j_1 \alpha_2 j_2 JM|T|\beta_1 j_1' \beta_2 j_2' JM\rangle \\
&= \sum_{m_1,m_2,\kappa_1,\kappa_2} \langle j_1 m_1, j_2 m_2|JM\rangle \langle j_1' m_1', j_2' m_2|J'M'\rangle (-1)^{j_1-m_1} \begin{Bmatrix} j_1 & k_1 & j_1' \\ -m_1 & \kappa_1 & m_1' \end{Bmatrix} \\
&\times (-1)^{j_2-m_2} \begin{Bmatrix} j_2 & k_2 & j_2' \\ -m_2 & \kappa_2 & m_2' \end{Bmatrix} \\
&\times \langle \alpha_1 j_1 m_1|T^{k_1}_{\kappa_1}|\beta_1 j_1' m_1'\rangle \langle \alpha_2 j_2 m_2|T^{k_2}_{\kappa_2}|\beta_2 j_2' m_2'\rangle.
\end{aligned}$$

We use Wigner-Eckart theorem again for $j_1,\ j_2,\ m_1$ and m_2 and obtain

$$\langle \alpha_1 j_1 \alpha_2 j_2 JM|T|\beta_1 j_1' \beta_2 j_2' JM\rangle = \hat{J}\hat{J}'\hat{k} \begin{Bmatrix} j_1 & j_2 & J \\ j_1' & j_2' & J' \\ k_1 & k_2 & k \end{Bmatrix} \langle \alpha_1 j_1|T_1|\beta_1 j_1'\rangle \langle \alpha_2 j_2|T(2)|\beta_2 j_2'\rangle,$$

where the symbols with a hat are defined as $\hat{I} = \sqrt{2I+1}$. The intermediate steps are omitted. For a complete derivation see for example Ref. [42].

8.2 Calculating the interactions

When computing the two-body matrix element

$$\langle k_1 k_2|v_{12}|k_1' k_2'\rangle,$$

it is convenient to perform the calculations in the relative and center-of-mass coordinates, where we define the relative momentum as

$$\mathbf{k} = \frac{1}{2}|\mathbf{k}_1 - \mathbf{k}_2| \tag{8.2}$$

and the center-of-mass momentum as

$$\mathbf{K} = (\mathbf{k}_1 + \mathbf{k}_2). \tag{8.3}$$

Since the potential is defined to be a function of the relative coordinates only, the interactions will be on the form

$$\langle kK|v(k,k')|k'K'\rangle = \langle k|v(k,k')|k'\rangle \delta_{K,K'}.$$

We need a method to transform the interactions in relative and center-of-mass-momenta to laboratory system. In quantum mechanics a general transformation is done by expanding our initially ket a in an orthonormal basis α.

$$|a\rangle = \sum_\alpha |\alpha\rangle\langle\alpha|a\rangle = \sum_\alpha \langle\alpha|a\rangle|\alpha\rangle.$$

In order to find the correct transformation we need to find the coefficients $\langle\alpha|a\rangle$. When computing the matrix element $\langle a|v|b\rangle$, we expand both the ket side and the bra side in the same orthonormal basis,

$$\langle a|v|b\rangle = \sum_{\alpha,\beta}\langle a|\alpha\rangle\langle\alpha|v|\beta\rangle\langle\beta|b\rangle.$$

We are now ready to make the transformations

$$\begin{aligned}|k_a l_a j_a k_b l_b j_b T_z J\rangle &= \sum_{l,L,j\mathcal{J}}\int d^3k\int d^3K \begin{Bmatrix} l_a & l_b & \lambda \\ \frac{1}{2} & \frac{1}{2} & S \\ j_a & j_b & J\end{Bmatrix} \\ &\times (-1)^{\lambda+\mathcal{J}-L-S}F\hat{\mathcal{J}}\hat{\lambda}^2\hat{j}_a\hat{j}_b\hat{S}\begin{Bmatrix} L & l & \lambda \\ S & J & \mathcal{J}\end{Bmatrix} \\ &\times \langle kljKL\mathcal{J},T_zJ|k_al_aj_ak_bl_bj_bT_zJ\rangle|kljKL\mathcal{J}T_zJ\rangle.\end{aligned} \tag{8.4}$$

The term $\langle kljKL\mathcal{J},T_zJ|k_al_aj_ak_bl_bj_bT_zK\rangle$ is the transformation coefficient from the relative system to the laboratory system. The factor F equals 1 for different particles $(T_z = 0)$ and $(1-(-1)^{l+S+T_z})/\sqrt{2}$ for identical particles. In our case the latter corresponds to either two neutrons or two protons that interact or a proton-neutron two-particle state. If we include isobars Δ, with isospin $3/2$, we may have coupled channels for different total values of spin S.

The problem is to find the transformation coefficients.
From Eqs (8.2) and (8.3) we obtain the relations

$$\begin{aligned}\mathbf{k}_1 &= -\mathbf{k}+\frac{K}{2} = \rho_1(\mathbf{k},\mathbf{K}) \\ \mathbf{k}_2 &= \mathbf{k}+\frac{K}{2} = \rho_2(\mathbf{k},\mathbf{K}).\end{aligned}$$

The two-particle bra state $\langle\mathbf{k}_1\mathbf{k}_2|$ is expanded in a partial wave basis as

$$\langle\mathbf{k}_1\mathbf{k}_2| = \frac{1}{k_1k_2}\sum_{l_1l_2\lambda\mu}\langle k_1l_1k_2l_2,\lambda\mu|\{Y^{l_1}(\hat{k}_1)\times Y^{l_2}(\hat{k}_2)\}.$$

The state $\langle\mathbf{kK}|$ is similar. We take the scalar product of $\langle\mathbf{kK}|$ and $|\mathbf{k}_1\mathbf{k}_2\rangle$ and get

$$\begin{aligned}\langle\mathbf{kK}|\mathbf{k}_1\mathbf{k}_2\rangle &= \frac{1}{kKk_1k_2}\sum_{\lambda\mu\lambda'\mu'}\sum_{lLl_1l_2}\{Y^l(\hat{k})\times Y^L(\hat{K})\}^\lambda_\mu \\ &\{Y^{l_1}(\hat{k}_1)\times Y^{l_2}(\hat{k}_2)\}^{\lambda'*}_{\mu'}\langle klKL,\lambda|k_1l_1k_2l_2.\lambda\rangle.\end{aligned} \tag{8.5}$$

By looking at the left side in the above equation we see that it obeys the two-particle state orthogonality relation

$$\langle\mathbf{kK}|\mathbf{k_1k_2}\rangle = \delta(\mathbf{k}_1-\rho_1(\mathbf{k},\mathbf{K}))\delta(\mathbf{k}_2-\rho_2(\mathbf{k},\mathbf{K})).$$

The explicit expression for the vector bracket $\langle \mathbf{k}l\mathbf{K}L,\lambda|\mathbf{k}_1 l_1 \mathbf{k}_2 l_2,\lambda\rangle$ can be obtained by multiplying each side of Eq. (8.5) with

$$\sum_{l_1 l_2 \lambda' \mu'} \{Y^{l_1'}(\hat{k}_1) \times Y^{l_2'}(\hat{k}_2)\}^{\lambda'*}_{\mu'} \{Y^{l_1'}(\hat{\rho}_1(\mathbf{k},\mathbf{K})) \times Y^{l_2'}(\hat{\rho}_2(\mathbf{k},\mathbf{K})\}^{\lambda'}_{\mu'},$$

and integrating over the solid angles $\hat{k}_1, \hat{k}_2, \hat{k}$ and $\hat{K}$ we finally obtain

$$\langle kljKL\mathcal{J}, T_z J|k_a l_a j_a k_b l_b j_b T_z K\rangle = \frac{4\pi^2}{kKk_a k_b}\delta(\omega)\theta(1-x^2)A(x),$$

with

$$\omega = k^2 + \frac{1}{4}K^2 - \frac{1}{2}(k_a^2 + k_b^2)$$
$$x = (k_a^2 - k^2 - \frac{1}{4}K^2)/kK,$$

and

$$A(x) = \frac{1}{2\lambda+1}\sum_{\mu}[Y^l(\hat{k}) \times Y^L(\hat{K})]^{\lambda*}_{\mu} \times [Y^{l_a}(k_a) \times Y^{l_b}(k_b)]^{\lambda}_{\mu}.$$

The functions Y are the spherical harmonics and x is the cosine angle between $\mathbf{k}$ and $\mathbf{K}$. From Eq. (8.4) we obtain the expression for the interactions in laboratory coordinates as

$$\begin{aligned}
&\langle k_a l_a j_a k_b l_b j_b T_z J|v|k_c l_c j_c k_d l_d j_d T_z J\rangle = \\
&\sum_{lLj\mathcal{J}l'} \int d^3k \int d^3K \int d^3k' \langle kljKL\mathcal{J}, T_z J|v|k'l'jKL\mathcal{J}T_z J\rangle \\
&\times \begin{Bmatrix} l_a & l_b & \lambda \\ \frac{1}{2} & \frac{1}{2} & S \\ j_a & j_b & J \end{Bmatrix} (-1)^{\lambda+\mathcal{J}-L-S} F\hat{\mathcal{J}}\hat{\lambda}^2 \hat{j}_a \hat{j}_b \hat{S} \begin{Bmatrix} L & l & \lambda \\ S & J & \mathcal{J} \end{Bmatrix} \\
&\times \langle kljKL\mathcal{J}, T_z J|k_a l_a j_a k_b l_b j_b T_z J\rangle \\
&\times \begin{Bmatrix} l_c & l_d & \lambda' \\ \frac{1}{2} & \frac{1}{2} & S' \\ j_c & j_d & J \end{Bmatrix} (-1)^{\lambda'+\mathcal{J}-L-S'} F\hat{\mathcal{J}}\hat{\lambda}'^2 \hat{j}_c \hat{j}_d \hat{S}' \begin{Bmatrix} L & l' & \lambda' \\ S' & J & \mathcal{J} \end{Bmatrix} \\
&\times \langle k_c l_c j_c k_d l_d j_d T_z J|k'l'jKL\mathcal{J}, T_z J\rangle.
\end{aligned} \tag{8.6}$$

8.3 Interactions again

In the last section we showed how to derive the interactions from relative coordinates. We observed that it is convenient to do the calculations in relative coordinates

because the interactions are diagonal in the center of mass coordinates and in relative angular momenta. We will now show how we find the orbital momentum dependency in the interactions. The interactions are on the form

$$\langle \mathbf{p}|v|\mathbf{k}\rangle.$$

We insert the completeness relation

$$\int d^3r|\mathbf{r}\rangle\langle\mathbf{r}| = I,$$

on both bra and ket side

$$\int d^3r \int d^3r'\langle \mathbf{p}|\mathbf{r}\rangle\langle\mathbf{r}|v|\mathbf{r}'\rangle\langle\mathbf{r}'|k\rangle. \tag{8.7}$$

For a local potential v, we write equation (8.7) as

$$\begin{aligned}\langle \mathbf{p}|v|\mathbf{k}\rangle &= \int d^3r\langle \mathbf{p}|\mathbf{r}\rangle\langle\mathbf{r}|v|\mathbf{r}\rangle\langle\mathbf{r}|\mathbf{k}\rangle \\ &= \frac{1}{(2\pi)^3}\int d^3re^{-i\mathbf{pr}}v(\mathbf{r})e^{i\mathbf{kr}},\end{aligned} \tag{8.8}$$

where we have inserted for the definition

$$\langle \mathbf{p}|\mathbf{r}\rangle = \frac{1}{(2\pi)^{\frac{3}{2}}}e^{-i\mathbf{pr}}.$$

In chapter 7 we showed how plane waves can be expanded in partial waves, we expand both of the exponentials in Eq. (8.8),

$$\frac{1}{(2\pi)^3}\int d^3r\sum_l(2l+1)i^lP_l(\Omega_{p,r})j_l(pr)\sum_{l'}(2l'+1)i^{l'}P_{l'}(\Omega_{k,r})j_{l'}(kr). \tag{8.9}$$

For a centrally symmetric potential, the interaction is on the form

$$\begin{aligned}&\frac{1}{2\pi^2}\int r^2dr\sum_l(2l+1)P_l(\Omega_{p,k})j_l(pr)vj_l(kr) \\ &= \frac{1}{2\pi^2}\sum_l(2l+1)P_l(\Omega_{p,k})\langle pl|v|kl\rangle,\end{aligned} \tag{8.10}$$

where we have used the orthogonality properties of the Legendre polynomials, see appendix D.1 for details. In the presence of a tensor force it is the total angular

momentum, j that is conserved and not the orbital momentum l. The interactions will be expressed as

$$\frac{1}{2\pi^2}\sum_{jll'}(2j+1)P_j(\Omega_{p,k})\langle pjl|v|kjl'\rangle. \tag{8.11}$$

For each j the orbital momentum in relative coordinates may have the values $|j-1|, j,$ and $j+1$. In our interactions we also included the total isospin, T_z, as a good quantum number.

Chapter 9

Results of the computations

The hardest task in doing the calculations was to write out the matrix elements to be read by another program that performs the coupled cluster calculations.
When operating in a plane wave basis we have both the mesh points for the numerical integration and the orbital angular momentum number l to consider, since we use a partial wave expansion of the wave function in a plane wave basis. The idea was to fix the maximum value of l to six, and the number of mesh points to 12. However it seemed that the maximum orbital angular momentum number had to be lowered to finish the thesis in time.

As we are doing the calculations with just two-body forces, and in a plane wave basis, the Hamiltonian is composed of the kinetic energy and a two-body interaction, defined as

$$H = \sum_{i=0}^{A} \frac{1}{2m}\langle i|k^2|i\rangle a_i^\dagger a_i + \frac{1}{2}\sum_{ijkl}\langle ij|v|kl\rangle a_i^\dagger a_j^\dagger a_l a_k.$$

When we integrate over momentum we are left with an undefined volume term Ω. We can overcome this problem by dividing with the number of particles. Technically this is done by dividing each energy term by the volume, Ω, and the density, ρ, defined in Eq. ((5.17)). We obtain then the expression

$$\sum_{jt_z}(2j+1)\int_0^{k_f}\frac{k^4}{2\pi^2}dk\frac{1}{2m_N\rho}+$$
$$\sum_{\substack{j_1 l_l 1 t_{z_1}\\ j_2 l_2 t_{z_2}}}\sum_{\substack{j_3 l_3 t_{z_3}\\ j_4 l_4 t_{z_4}}}(2J+1)\int\frac{d^3k_1 d^3k_2 d^3k_3 d^3k_4}{(2\pi)^{12}\rho}\langle j_1 l_1 k_1 t_{z_1} j_2 l_2 k_2 t_{z_2} JT_z|v|j_3 l_3 k_3 t_{z_3} j_4 l_4 k_4 t_{z_4} JT_z\rangle.$$

In a numerical calculation the integrals over k are approximated by finite sums over the number of mesh points N

$$\int f(k)k^2dk \rightarrow \sum_i^N f(k_i)k_i^2\omega_i,$$

where k_i and ω_i are the integration points (mesh points) and integration weights, respectively. In performing the integrals numerically we employed Gaussian quadrature (with Legendre polynomials), for details see [43].

The nuclear interaction model used is the chiral N^{3}LO version of Entem and Machleidt [44] with an interaction cutoff $\Lambda = 500$ MeV. We renormalized the N^3LO potential using the similarity transformation in momentum space described earlier. This interaction is labelled V_{low-k} with model spaces defined by the different values of the cutoff λ[1]. We have employed the following values of the cutoff 2.1 fm^{-1}, 2.2 fm^{-1} and 2.5 fm^{-1}.

Most nuclear matter calculations have been done with a perturbational approach, starting with renormalizing the potential with for example a similarity transformation method in momentum space, yielding the so-called V_{low-k} renormalization scheme. The Brueckner G-matrix approach is also an often used as starting point for nuclear matter computations. It is a way to circumvent the strictly non-perturbative part of the nuclear interactions. It is briefly described in appendix C.

9.1 The programs

Two separate programs were used, one which calculates the interaction elements in the laboratory frame and another program which performs the coupled cluster computations. As mentioned above, the hardest task was to compute the interactions. This part is rather time-consuming due to the computation of the vector-bracket coefficients. In order to improve the efficiency it had to be parallelized. It was not so difficult to parallellize the program since one interaction element does not depend on the other elements. The computation of the interaction elements was spread out evenly on different processes. The pseudo-code below shows how a for-loop was parallelized.
Complications arose when the interaction elements were written to the file to be read

[1]Note well that the cutoff in the model space is not the same as the cutoff used in chiral perturbation theory to define the nucleon-nucleon interaction.

```
for i= iam+1, n, numprocs do
   some code
end for
```

by the coupled cluster program. The easiest way was to let each process write their matrix elements to their own file and then concatenate the files to one. This is a rather fast process but it generates many files and is not always easily implemented on the supercomputing clusters (Titan@uio.no and Hexagon@uib.no) which we had access to in this thesis work. What was done was to let each process store their interaction elements in an array which was sent to the master node, which then writes them to file. This is a rather tedious and slow process and it is not recommended.

A better method would be to use the MPI I/O functions which let the different processes write to the same file. The complications which made us avoid the MPI I/O method was that we needed to know both the total file size and the size of the files that each process needs. Because of the bracket transformations it was difficult to know how much each process would need to write. We came to the conclusion that if we gave the processes a too huge size of the file than necessary, it could generate blank lines, which may yield problematic when reading it. Another MPI tool to use is NETCDF4/HDF5, however with this it was difficult to write the matrix elements in the form the coupled cluster program demands.

The coupled cluster program used was originally written in a harmonic oscillator basis. Some minor changes in how the program reads the interaction elements had to be done in order to make the coupled cluster program work in a plane wave basis as well. In order not to change the program too much the matrix elements to be read were already multiplied with the mesh points and weights for the integrations

$$\begin{aligned}&\langle l_1 j_1 k_2 l_2 k_2 JT_z|v|l_3 j_3 k_3 l_4 j_4 k_4 JT_z\rangle \\ &\rightarrow \langle l_1 j_1 k_1 l_2 j_2 k_2 JT_z|v|l_3 j_3 k_3 l_4 j_4 k_4 JT_z\rangle k_1 k_2 k_3 k_4 \sqrt{w_1 w_2 w_3 w_4}.\end{aligned}$$

Then the only thing needed was to multiply with the factor $1/(2\pi)^2$ for each integration variable and keep in mind that nothing should be divided by the weights and mesh points when solving for the cluster amplitudes.

9.2 Results

The aim of the thesis was to calculate the binding energy of symmetric nuclear matter and obtain an equation of state of pure neutron matter with the coupled cluster method. As this was done in a plane wave basis, we had to do an integration over momentum, k, in the region where $k \in [0, \infty]$. Numerically this is accomplished by a tangential mapping. As the renormalization scheme V_{low-k} was used, the problem is projected to a smaller space by defining $k \in [0, \lambda]$, where λ usually ranges from 2 fm^{-1} to 3 fm^{-1}. The tangential projection procedure was omitted since the mesh-points were projected onto the new interval $k \in [0, \lambda]$.

In chapter 7 we saw that when doing coupled cluster calculation we have to make a distinction between particles and holes. In chapter 3 we defined holes as particles inside the Fermi sphere and particles to be outside. The radius of the Fermi sphere was set to be k_f where k_f ranges from 1.2 fm^{-1} to 1.9 fm^{-1}. All single-particle states with a momentum below or equal k_f are to be holes and those with a momentum greater than k_f were defined as particles.

In Fig. 9.1 we present the first-order energies for orbital angular momentum, l, values truncated at four and six. The saturation density remains more or less constant for both l-values at 1.75 fm^{-1}, which is greater than the experimental value at 1.42 fm^{-1}. The binding energy, approximately 3MeV, is way too low for orbital angular momentum truncated at four, compared to the experimental value, 16 MeV. For $\lambda = 2.5$ fm^{-1} the first order approximation failed to give a minimum within the range of k_f studied by us.

An interesting observation is that the cutoff $\lambda = 2.1$ fm^{-1} gives a higher binding energy (lower minimum) than the cutoff on 2.2 fm^{-1}. This is because the interaction elements with lower λ have higher absolute values. This will of course have an effect on the coupled cluster computations as well. By including three-body forces we should be able to correct for this dependency on the cutoff. In Fig. 10.1 we present a work on nuclear matter with three-body forces by [45]. We see that by including three-body forces the interactions become less cutoff dependent.

The first-order calculations with angular momentum truncated at $l = 6$ and $\lambda = 2.2$ almost reproduce the experimental binding energy, but with a lower cutoff the interaction elements get higher and fail to reproduce the experimental binding energy, as can be seen in Fig. 9.1. The cutoff in momentum $\lambda = 2.5$ fm^{-1} fails to give a minima in our range of k_f. We have again an indication for the need of three-body forces. Coupled cluster computation on $l = 6$ were not completed since they were very time consuming and required too much memory to be run on Hexagon@uib.no.

$\lambda = 2.1$ fm^{-1}			$l_{\max} = 4$		
k_f	Total energy	$\sum_{ai} f_{ai} t_i^a$	$\sum_{abij} v_{abij} t_i^a t_j^b$	$\sum_{abij} v_{abij} t_{ij}^{ab}$	Total correction
1.2	3.787507	-0.030488	-0.000117	-0.058656	-0.089261
1.4	3.82199	-0.030239	-0.000889	-0.145316	-0.175644
1.6	-2.071725	-0.057642	-0.000140	-0.113498	-0.171280
1.8	-4.307874	-0.117001	-0.000423	-0.058656	0.176080
1.9	0.215606	-0.05693	-0.000129	-0.032594	-0.089660
$\lambda = 2.2$ fm^{-1}			$l_{\max} = 4$		
k_f	Total energy	$\sum_{ai} f_{ai} t_i^a$	$\sum_{abij} v_{abij} t_i^a t_j^b$	$\sum_{abij} v_{abij} t_{ij}^{ab}$	Total correction
1.2	2.856008	-0.025748	-0.000100	-0.153787	-0.179635
1.4	3.664643	-0.026888	-0.000006	-0.175784	-0.202737
1.6	1.429075	-0.075102	-0.000432	-0.184876	-0.260410
1.7	-4.663540	-0.186931	-0.002106	-0.169220	-0.358257
$\lambda = 2.5$ fm^{-1}			$l_{\max} = 4$		
1.4	6.426474	0.001282	0.000037	-0.322986	-0.321667

Table 9.1: Energies and correction to the first order energy for different values of λ and k_f. All energies are in MeV

In the case of pure neutron matter the equation of state is almost constant as a function of the cutoff, as can be seen in Fig. 9.2. In neutronmatter the tensor force is insignifant and there are less hole-hole and particle-particle correlations which may explain this independency.

In Fig. 9.3 we present coupled cluster calculations for symmetric nuclear matter and pure neutron matter. In table 9.1 we summarize the coupled cluster calculations on symmetric nuclear matter. We observe that the corrections to the first-order approximation increases with the cutoff, λ. The model space becomes smaller and there are fewer intermediate states when the cutoff is lowered. We used an ordinary linear iteration scheme to solve the amplitude equations and that can be a reason for why some values failed to converge, such as for $k_f = 1.8$ with cutoff $\lambda = 2.2$fm^1 and $\lambda = 2.5$fm^{-1}.

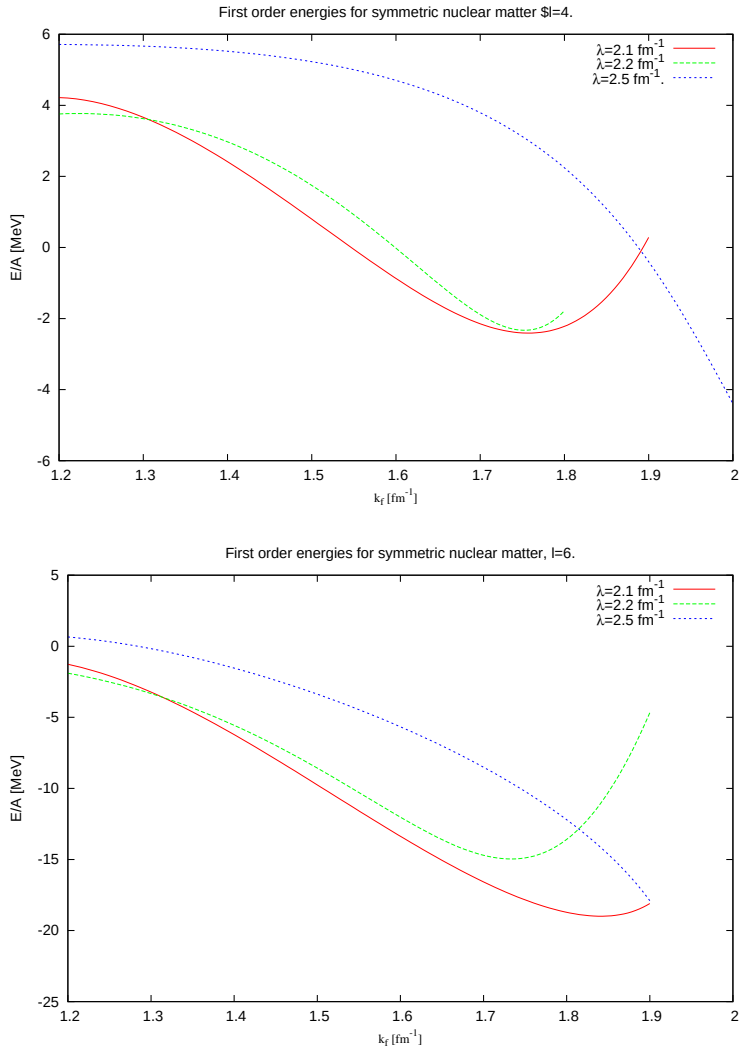

Figure 9.1: The diagrams depict first-order energies for symmetric nuclear matter. The upper diagram has orbital angular momentum truncated at $l = 4$. The lower is truncated at $l = 6$ both with cutoffs $\lambda = 2.1\text{fm}^{-1}$, $\lambda = 2.2\text{fm}^{-1}$ and $\lambda = 2.5$ fm^{-1}.

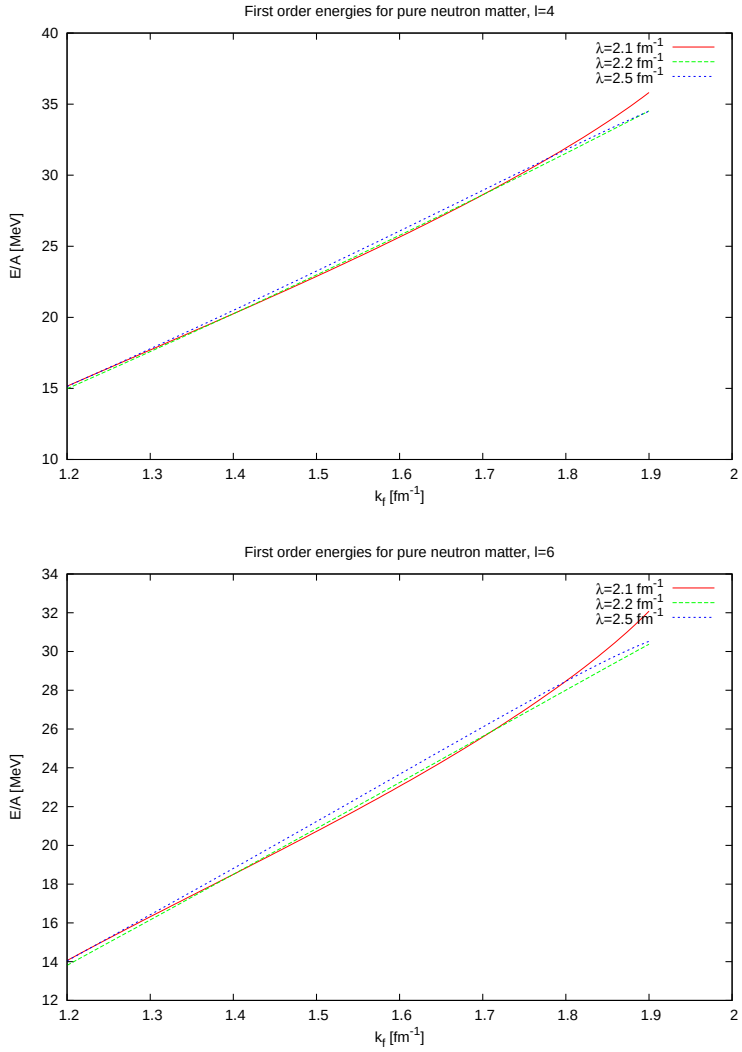

Figure 9.2: The diagrams depict first-order equation of state for pure neutron matter. In the upper diagram the orbital angular momentum is truncated at $l = 4$. In the lower diagram the orbital momentum is truncated at $l = 6$ both with cutoffs $\lambda = 2.1\text{fm}^{-1}$, $\lambda = 2.2\text{fm}^{-1}$ and $\lambda = 2.5$ fm^{-1}.

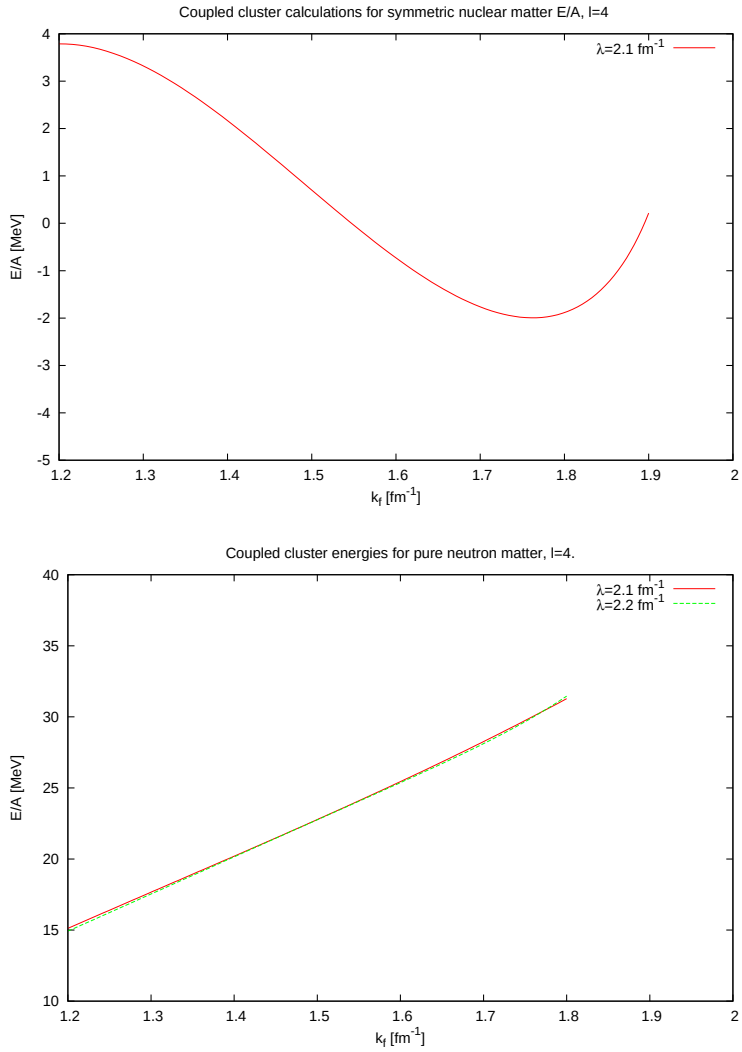

Figure 9.3: Coupled cluster calculations, the upper diagram shows energy for symmetric nuclear matter. The lower diagram depicts the equation of state of pure neutron matter. Both calculations are done with orbital momentum truncated at $l = 4$. The upper diagram has cutoff $\lambda = 2.1\text{fm}^{-1}$, while the lower with $\lambda = 2.1$ and $\lambda = 2.2$.

Chapter 10

Conclusion

In this thesis we did coupled cluster calculation on both symmetric nuclear matter and pure neutron matter. The equation of state of nuclear matter is an important factor in the studies of nuclear properties, heavy ion collisions, neutron stars and supernovae. By using the coupled cluster method we can calculate binding energies by first principles. The only inputs we need in the theory are the interactions.

We can affirm that it is possible to perform coupled cluster calculations on nuclear matter and we have obtained an explicit convergence at least for the cutoff $\lambda = 2.1$ fm^{-1}. For the cases without convergence as for $k_f = 1.8$ fm^{-1} with $\lambda = 2.2$ fm^{-1}, $\lambda = 2.5$ fm^{-1} may be as a consequence of the primitive linear iteration scheme. As expected the convergence is faster for a smaller cutoff. This is due to the fact that with a larger cutoff we expect more contributions from intermediate particle-particle states, as can be seen from table 9.1. The model space is smaller and we have fewer particle states with small cutoffs. However, we must admit that some of the results were not as expected, the corrections to the first-order energy were expected to be higher, and we also notice that it seems that the first-order energy blows up by including more orbital angular momenta in the laboratory system.

From Fig. 9.1 we see that in the nuclear matter case the energy density depends strongly on choice of cutoff. When we do a similarity transformation the absolute values of the new interaction elements become higher. A lower cutoff increases the absolute value of the interaction elements and we therefore expect stronger bindings.

In the case of pure neutron matter the energies are almost independent of the cutoff. In neutronmatter the tensor force is insignificant which yields fewer hole-hole and particle-particle correlations and we have therefore small differences in the energies computed.

From table 9.1 and Figs. 9.1 and 9.3 we see that the truncation on $l = 4$ is too low to give a good estimate for the binding energy of symmetric nuclear matter. The truncation on $l = 6$ is closer to the experimental value but we need three-body forces and relativistic corrections if we want a more realistic approach.

It may seem that we need a better understanding of the nuclear interactions. In Ref. [46] they claim that most of the theoretical calculations on the binding energy of nuclear matter overbind the system up to 25%, however some calculations also underbind the system, which may indicate a lack of understanding the nucleon-nucleon interactions. We also observe that the corrections to the energy is higher for a larger cutoff λ. This may indicate that the intermediate states contribute more. We "lose" physical correlations when the cutoff is lowered.

An improvement to the project and the coupled cluster calculations could be to include relativistic effects and three-body interactions. In [45] there were done calculations with three-body forces where they managed to reduce the cutoff dependency. In Fig. 10.1 we present some of the calculations done by [45] on nuclear matter with three-body forces. In Fig. 10.2 they compare results by including three-body forces and calculations with only two-body-forces. We see that with two-body forces only they fail to reproduce a minimum in the range of their calculations and that there is a significant cutoff dependency, as in our case.

It would also be convenient to make the coupled cluster program more efficient. The interaction files are huge and require much memory when the program stores the interactions in arrays.

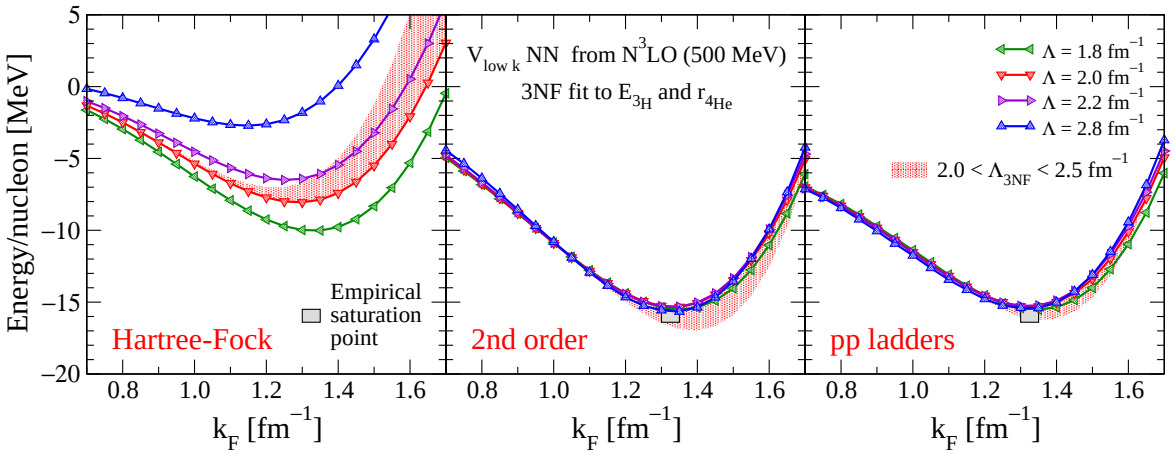

Figure 10.1: (Color online) Nuclear matter energy per particle as a function of Fermi momentum k_f at the Hartree-Fock level (left) and including second-order (middle) and particle-particle-ladder contributions (right), based on evolved N^{3}LO NN potentials and 3NF fit to $E_{^3\mathrm{H}}$ and $r_{^4\mathrm{He}}$. Theoretical uncertainties are estimated by the NN (lines) and 3N (band) cutoff variations.

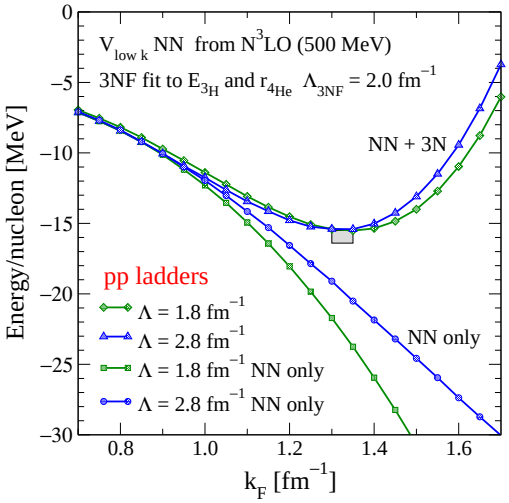

Figure 10.2: (Color online) Nuclear matter energy of Fig. 10.1 at the particle-particle-ladders level compared to NN-only results for two representative NN cutoffs and a fixed 3N cutoff.

Appendix A

Diagram rules

1. There are $n+1$ vertices, one vertex for each time, with the ordering $t < t_1 < t_2 < \cdots < t_n$. Each vertex/interaction is represented by a dashed line, as in Fig. 4.2.

2. Lines with upward pointing arrows are particles and lines with downward pointing arrows are holes. Lines starting and ending at the same vertex are holes.

3. Each vertex gives a factor $\frac{1}{2}V_{\alpha\beta\gamma\delta}$.

4. There is an overall sign $(-1)^{n_h+n_l}$, where n_h is the number of hole lines and n_l is the number of fermion loops.

5. For each interval between two successive vertices there is an energy factor

$$\left[\sum_h \epsilon_h - \sum_p \epsilon_p\right]^{-1},$$

   where the sum over h is over all hole lines in the interval and the sum over p is over all particle lines in the interval.

6. For each pair of lines that begins at the same interaction line and ends at the same interaction line gives a factor $1/2$.

7. All the above factors have to be multiplied together and summing over all labels of fermion lines.

Appendix B

Plane waves and spherical waves

When transforming the potential to momentum basis, it is very useful to use an expansion for the product $\langle \mathbf{x}|\mathbf{k}\rangle$. In order to get this transformation we will have to look at both plane waves, spherical waves and the connection between these two. In a free particle state the Hamiltonian consists just of the kinetic energy operator, and obviously also commutes with the momentum operator, with the eigenvalue $\mathbf{k}$. The free particle Hamiltonian commutes also with the operators $\mathbf{L}^2$ and L_z, we can then find an eigenket of $H_0, \mathbf{L}^2$ and L_z denoted $|Elm\rangle$, here the spin is suppressed. This state is called a spherical wave state. As a free state can be regarded as a superposition of various plane wave states $|\mathbf{k}\rangle$ with different $\mathbf{k}$, the same can be done with spherical wave states, but here with various E, l and m. A free particle state can be analyzed by plane wave states or spherical wave states.

There should be a connection between a plane wave basis and a spherical wave basis, this connection which may transform a plane wave basis to a spherical wave basis will be derived. Since the complete spherical wave basis is orthonormal each state satisfies the condition

$$\langle E'l'm'|Elm\rangle = \delta_{ll'}\delta_{mm'}\delta(E' - E).$$

Since we have an complete basis we can expand a plane wave state in a spherical wave basis as

$$|\mathbf{k}\rangle = \sum_{lm} \int dE \langle Elm|\mathbf{k}\rangle |Elm\rangle.$$

We need to find the transformation coefficient $\langle Elm|\mathbf{k}\rangle$. It is helpful to first consider a plane wave state whose propagation is along the z axis, $|k\hat{\mathbf{z}}\rangle$. A crucial property of this state is that there is no orbital momentum in the z direction

$$L_z|k\hat{\mathbf{z}}\rangle = 0.$$

The expansion of $|k\hat{\mathbf{z}}\rangle$ is

$$|k\hat{\mathbf{z}}\rangle = \sum_l \int dE|E,l,m=0\rangle\langle E,l,m=0|k\hat{\mathbf{z}}\rangle \tag{B.1}$$

A general eigenket $|\mathbf{k}\rangle$ can be obtained by applying a rotation operator on Eq. (B.1),

$$|\mathbf{k}\rangle = \mathcal{R}|k\hat{\mathbf{z}}\rangle.$$

Let us now multiply $\langle Elm|$ with $|\mathbf{k}\rangle$,

$$\begin{aligned}\langle Elm|\mathbf{k}\rangle &= \sum_{l'} \int dE'\langle Elm|\mathcal{R}|E',l',m'=0\rangle\langle E',l',m'=0|k\hat{\mathbf{z}}\rangle \\ &= \sum_{l'} \int dE'\mathcal{R}^l_{m0}\delta_{ll'}\delta(E-E')\langle E',l',m'=0|k\hat{\mathbf{z}}\rangle \\ &= \mathcal{R}^l_{m0}\langle Elm=0|k\hat{\mathbf{z}}\rangle.\end{aligned}$$

In order to solve this we observe that the coefficient $\langle Elm=0|k\hat{\mathbf{z}}\rangle$ is independent of the angles θ and ϕ. We can then postulate that it is on the form $\sqrt{2l+1/4\pi}g_{lE}*(k)$. Since the spherical harmonics Y^m_l are defined as $\sqrt{2l+1/4\pi}\mathcal{R}^l_{m0}$. We can write the transformation coefficient $\langle\mathbf{k}|Elm\rangle$ as

$$\langle\mathbf{k}|Elm\rangle = g_{lE}(k)Y^m_l(\hat{\mathbf{k}}).$$

The function $g_{lE}(k)$ is the last part to determine. This is done by observing that

$$(H_0 - E)|Elm\rangle = 0,$$

and by doing the same on the eigenbra $\langle\mathbf{k}|$ we obtain

$$\langle\mathbf{k}|(H_0-E) = \langle\mathbf{k}|\left(\frac{k^2}{2m} - E\right).$$

Multplying $|Elm\rangle$ from the right gives zero,

$$\left(\frac{k^2}{2m} - E\right)\langle\mathbf{k}|Elm\rangle = 0.$$

It follows that $\langle\mathbf{k}|Elm\rangle$ is only nonvanishing when

$$E = \frac{k^2}{2m}.$$

We can then write

$$g_{lE}(k) = N\delta(\frac{k^2}{2m} - E),$$

where N is a normalization constant which can be found by considering the orthonormalization condition for $\langle E'l'm'|Elm\rangle$. It turns out that

$$N = \frac{1}{\sqrt{mk}}.$$

And hence

$$\langle \mathbf{k}|Elm\rangle = \frac{1}{\sqrt{mk}}\delta(\frac{k^2}{2m} - E)Y_l^m(\hat{\mathbf{k}}). \tag{B.2}$$

In order to get the transformation in coordinate space we have to use the fact that the wave function for a free spherical wave is $j_l(kr)Y_k^m(\hat{\mathbf{r}})$, where $j_l(kr)$ is the spherical Bessel function of order l.

The transformation coefficient $\langle \mathbf{x}|Elm\rangle$ is then on the form

$$\langle \mathbf{x}|Elm\rangle = c_l j_l(kr)Y_l^m(\hat{\mathbf{r}}), \tag{B.3}$$

where c_l has to be determined. It is determined by comparing Eq. (B.3) with $\langle \mathbf{x}|\mathbf{k}\rangle$. We find that $c_l = i^l\sqrt{2mk/\pi}$.

Appendix C

Brueckner G-matrix

The Brueckner G-matrix is one of the most important ingredients in many-body calculations. The G-matrix was developed for microscopic nuclear matter calculations, [47, 48]. It is a method to overcome the non perturbative character of the nuclear force, caused by the short range repulsive core in the NN interaction.

We want to calculate the nuclear matter ground state energy by using the non-relativistic Hamiltonian

$$H\Psi_0(A) = E_0\Psi_0(A),$$

where $H = T + V$ and A denotes the particle number, T is the kinetic energy and V is the nucleon-nucleon potential. The unperturbed problem, is

$$H_0\psi_0(A) = W_0\psi_0(A).$$

In this case, H_0 consists just of the kinetic energy, and ψ_0 is a Slater determinant representing the Fermi sea. The full ground state energy, E_0 is

$$E_0 = W_0 + \Delta E_0,$$

where ΔE_0 is the ground state energy shift and is the value we need to find, since W_0 is easily obtained. The energy shift is normally found with perturbation theory. When the the potential $V(r)$ contains a strong short-range repulsive core, the matrix elements containing V will become very large and contribute repulsive to the ground state energy. Thus it is meaningless to treat the problem with perturbation theory.

The resolution to this problem, was provided by Brueckner by introducing a matrix, the so-called G-matrix. It can be compared with the function $f(x) = x/(1-x)$, this function may be expanded in the series $f(x) = x+x^2+x^3+\cdots$ when x is small, and it is not necessary to compute all terms if we want an approximation. If x is large, the power series become meaningless, but the exact function

$x/(1-x)$ is still well defined. Brueckner suggested that one should sum up all terms in the perturbative approach, this sum is denoted by G_{ijij}, where $G_{ijij} = \langle ij|G|ij\rangle$. The expression for G is

$$G_{ijij} = V_{ijij} + \sum_{mn>k_f} V_{ijmn}\frac{1}{\varepsilon_i + \varepsilon_j - \varepsilon_m - \varepsilon_n} \times \left(V_{mnij} + \sum_{pq>k_f} V_{mnpq}\frac{1}{\varepsilon_i + \varepsilon_j - \varepsilon_p - \varepsilon_q}V_{pqij}\right).$$

Which we again can write as

$$G_{ijij} = V_{ijij} + \sum_{mn>k_f} V_{ijmn}\frac{1}{\varepsilon_i + \varepsilon_j - \varepsilon_m - \varepsilon_n}G_{mnij}$$

The matrix elements become $\langle\psi|G|\psi\rangle = \langle\psi|V|\Psi\rangle$. Where Ψ is the correlated wave function. When it is not possible to solve for the G-matrix with matrix inversion it is done by an iterative approach.

It is useful to write the G-matrix in a more general form

$$G_{ijij} = V_{ijij} + \sum_{mn>0} V_{ijmn}\frac{Q(mn)}{\omega - \varepsilon_m - \varepsilon_n}G_{mnij}.$$

The factor $Q(mn)$ corresponds to

$$Q(k_m, k_n) = \begin{cases} 1 & \min(k_m, k_n) > k_f \\ 0 & \text{else} \end{cases}$$

The role of Q is to enforce the Pauli principle by preventing scattering to occupied states. The G-matrix can be written on a more compact form, by noticing

$$H_0|\psi_m\psi_n\rangle = (\varepsilon_m + \varepsilon_n)|\psi_m\psi_n\rangle,$$

to

$$G(\omega) = V + V\frac{Q}{\omega - H_0}G(\omega),\ Q = \sum_m |\psi_m\psi_n\rangle Q(mn)\langle\psi_m\psi_n|.$$

If the Pauli exclusion operator, Q, does not commute with the Hamiltonian H_0 we have to do the replacement

$$\frac{Q}{\omega - H_0} \to Q\frac{1}{\omega - H_0}Q.$$

There are a number of complexities with the calculation of the G-matrix, we have already mentioned one, when the Q does not commute with H_0, the determination of the starting energy ω may also be a problem.

Appendix D

Special functions

D.1 Legendre polynomials

The Legendre functions are solutions of the differential equation

$$\frac{d}{dx}\left[(1-x^2)\frac{d}{dx}P(x)\right] + l(l+1)P(x) = 0, \tag{D.1}$$

and by using Rodrigues' formula expressed as

$$P_l(x) = \frac{1}{2^l l!}\frac{D^l}{dx^l}(x^2-1)^l. \tag{D.2}$$

The Legendre polynomials satisfy an orthogonality property on the interval $-1 \leq x \leq 1$,

$$\int_{-1}^{1} dx P_l(x)P_k(x) = \frac{2}{2l+1}\delta_{lk}.$$

The Legendre polynomials for $l = 0, \cdots, 5$ are

l	$P_l(x)$,
0	1,
1	x,
2	$\frac{1}{2}(3x^2-1)$,
3	$\frac{1}{2}(5x^3-3x)$,
4	$\frac{1}{8}(35x^4-30x^2+3)$,
5	$\frac{1}{8}(63x^5-70x^3+15x)$.

D.2 Spherical Bessel functions

The spherical Bessel functions are solutions of the radial part of the differential equation

$$x^2\frac{d^2y}{dx^2} + x\frac{dy}{dx} + (x^2 - \alpha^2)y = 0$$

using spherical coordinates by separation of variables. There are two linearly independent sets of solution to this equation $j_l(x)$ and $y_l(x)$, they are related to the ordinary Bessel functions J_l and Y_l by

$$j_n(x) = \sqrt{\frac{\pi}{2x}}J_{n+1/2}(x), \tag{D.3}$$

and

$$y_n(x) = \sqrt{\frac{\pi}{2x}}Y_{n+1/2}(x) = (-1)^{n+1}\sqrt{\frac{\pi}{2x}}J_{-n-1/2}(x).$$

In our calculation we have only used the spherical Bessel functions of first kind j_l and they can be expressed as

$$j_n(x) = (-x)^n\left(\frac{1}{x}\frac{d}{dx}\right)^n\frac{\sin x}{x}. \tag{D.4}$$

While the spherical Bessel function of second kind can be expressed as

$$y_n(x) = -(-x)^n\left(\frac{1}{x}\frac{d}{dx}\right)^n\frac{\cos x}{x}.$$

The first four spherical Bessel functions of first kind are

$$\begin{aligned}
j_0(x) &= \frac{\sin x}{x},\\
j_1(x) &= \frac{\sin x}{x^2} - \frac{\cos x}{x},\\
j_2(x) &= \left(\frac{3}{x^2} - 1\right)\frac{\sin x}{x} - \frac{3\cos x}{x^2},\\
j_3(x) &= \left(\frac{15}{x^3} - \frac{6}{x}\right)\frac{\sin x}{x} - \left(\frac{15}{x^2} - 1\right)\frac{\cos x}{x}.
\end{aligned}$$

Bibliography

[1] A. Hewish, J. Bell, J. D. H. Pilkington, P. F. Scott, and R. A. Collins, Nature **217**, 709 (1968).

[2] B. D. Day and J. G. Zabolitsky, Nucl. Phys. A **366**, 221 (1981).

[3] C.-L. Kung, *The effect of high energy excitations in the core polarization diagram in mass 18 nuclei*, PhD in physics, State University of New York at Stony Brook, 1978.

[4] T. D. Crawford and H. F. SchaeferIII, Reviews in Computational Chemistry **14**, 33 (2000).

[5] R. J. MacKay and R. W. Oldford, Statistical Science **15**, 254 (2000).

[6] S. S. Afshar, PROC.SPIE **5866**, 229 (2005).

[7] S. S. Afshar, AIP CONF.PROC. **810**, 294 (2006).

[8] A. L. Fetter and J. D. Walecka, *Quantum Theory of Many-Particle Systems* (Dover publications, 2003).

[9] E. K. U. Gross, E. Runge, and O. Heinonen, *Many-Particle Theory* (Adam Hilger, Bristol, 1991).

[10] M. Hjorth-Jensen, T. T. Kuo, and E. Osnes, Physics Reports **261**, 125 (1995).

[11] D. J. Thouless, *Quantum Mechanics of Many Body Systems* (Academic Press, 1961).

[12] R. Shankar, *Principles of Quantum Mechanics* (Springer, 1994).

[13] J. J. Sakurai, *Modern Quantum Mechanics*, (Addison Wesley, 1993).

[14] T. T. S. Kuo, *Topics in many-body theory of nuclear effective interactions*, Lecture Notes in Physics Vol. 144 (Springer, 1981).

[15] P. J. Siemens and A. S. Jensen, *Elements of nuclei* (Addison Wesley Publishing, 1987).

[16] K. S. Krane, *Introductory nuclear physics* (John Wiley & Sons, 1988).

[17] S. Abachi *et al.*, Phys. Rev. Lett. **74**, 2422 (1995).

[18] F. Abe *et al.*, Phys. Rev. Lett. **74**, 2626 (1995).

[19] H. Yukawa, Proc. Phys.-Math. Soc. Japan **17**, 48 (1935).

[20] R. Machleidt, Nuclear forces from chiral effective field theory, 2007, `http://www.citebase.org/abstract?id=oai:arXiv.org:0704.0807`.

[21] M. E. Peskin and D. V. Schroeder, *An Introduction to Quantum Field Theory* (Westview Press, 1995).

[22] S. Scherer and M. R. Schindler, A chiral perturbation theory primer, 2005, `http://www.citebase.org/abstract?id=oai:arXiv.org:hep-ph/0505265`.

[23] E. Epelbaum, Prog. Part. Nucl. Phys. **57**, 654 (2006).

[24] M. Hjorth-Jensen, lecture1, Lecture notes in physics, `http://folk.uio.no/mhjensen/manybody/cens1.pdf`

[25] F. Mandl and G. Shaw, *Quantum Field Theory* (Wiley, 1993).

[26] S. Weinberg, *The Quantum Theory of Fields, Volume 1: Foundations* (Cambridge University Press, 2005).

[27] I. Aitchison and A. Hey, *Gauge Theories in Particle Physics*, (Taylor & Francis, 2004).

[28] S. K. Bogner, T. T. S. Kuo, and A. Schwenk, Phys. Rep **386**, 1 (2003).

[29] A. Zee, *Quantum Field Theory in a Nutshell* (Princeton University Press, 2003).

[30] G. Hagen, M. Hjorth-Jensen, and N. Michel, Phys. Rev. C **73**, 064307 (2006).

[31] C. Bloch, Nucl. Phys. **6**, 329 (1958).

[32] C. Bloch and J. Horowitz, Nucl. Phys. **8**, 91 (1958).

[33] K. Suzuki and S. Y. Lee, Prog. Theo. Phys. **64**, 2091 (1980).

[34] S. Y. Lee and K. Suzuki, Phys. Lett. B **91**, 173 (1980).

[35] B. K. Jennings, Europhysics Letters **72**, 211 (2005).

[36] F. Coester, Nuclear Physics **7**, 421 (1958).

[37] F. Coester and H. Kümmel, Nucl. Phys. **17**, 477 (1960).

[38] T. Kuo, J. Shurpin, K. Tam, E. Osnes, and P. Ellis, Ann. phys. **132**, 237 (1981).

[39] A. de Shalit and I. Talmi, *Nuclear shell theory* (Academic Press New-York, 1963).

[40] R. J. Bartlett and M. Musial, Rev. Mod. Phys. **79**, 291 (2007).

[41] G. Hagen *et al.*, Phys. Rev. C **76**, 034302 (2007).

[42] K. L. Heyde, *The nuclear shell model* (Springer, 1990).

[43] M. Hjorth-Jensen, Computational physics, Lecture notes, `www.uio.no/studier/emner/matnat/fys/FYS3150/h07/undervisningsmateriale/Lecture%20Notes/lecture2007.pdf`.

[44] D. R. Entem and R. Machleidt, Phys. Rev. C **68**, 041001 (2003).

[45] S. K. Bogner, R. J. Furnstah, A. Nogga and A. Schwenk Nuclear matter from chiral low-momentum interactions, `http://www.citebase.org/abstract?id=oai:arXiv.org:0903.3366`

[46] V. Soma and P. Bozek, Phys. Rev. C **78**, 054003 (2008).

[47] K. A. Brueckner, Phys. Rev. **97**, 1353 (1955).

[48] H. A. Bethe, B. H. Brandow, and A. G. Petschek, Phys. Rev. **129**, 225 (1963).